

Guided combinatorial synthesis, high-throughput characterization and machine learning expedite discovery of improved Pt-Au thin films

D.P. Adams, R. Kothari, T. Shilt, S. Desai, C. Sobczak,
J. Custer, M. Kalaswad, K. Dorman, S. Addamane, N. Bianco, M. Jain,
E. Fowler, F. DelRio, M. Rodriguez, C. Martinez, R. Dingreville, B. Boyce

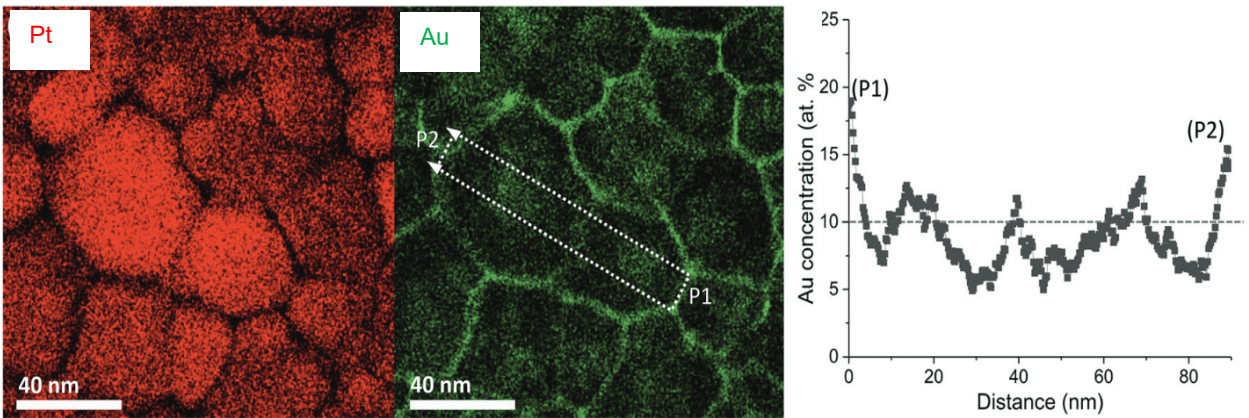
Sandia National Laboratories

PacSurf

December, 2024

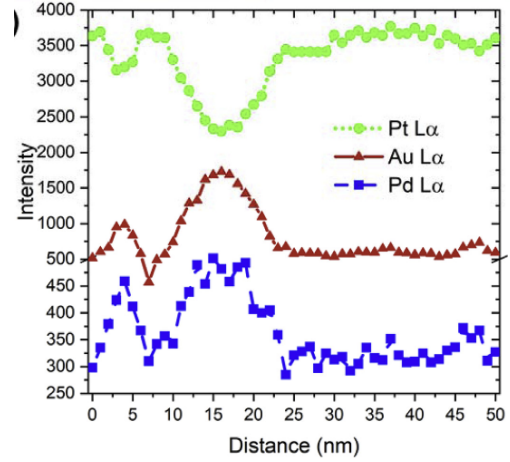
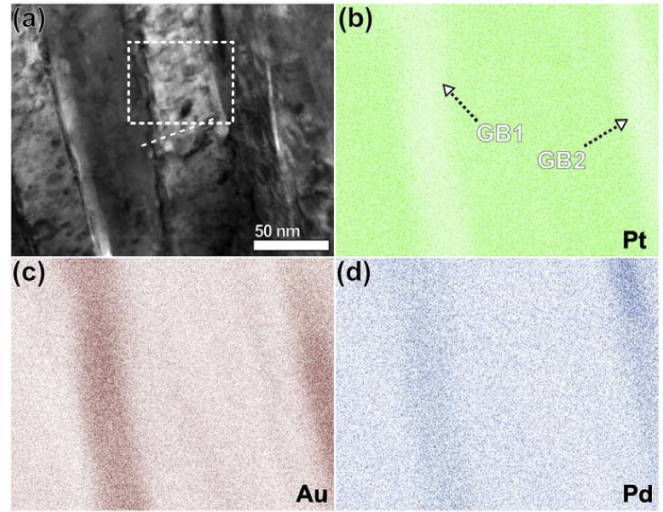


Several binary and ternary metal alloys exhibit nanocrystalline structures w/ compositional segregation.



Au at grain boundaries !!

Ex. 1 Sputter-deposited $Pt_{0.9}Au_{0.1}$ (after annealing 500C) exhibits compositional segregation (Nanoscale, 2021 Bahr et al.)



Au & Pd at grain boundaries !!

Ex. 2 PdAuPt Thin Film - annealed 400C (Acta Materialia, 2018, Xing et al.)

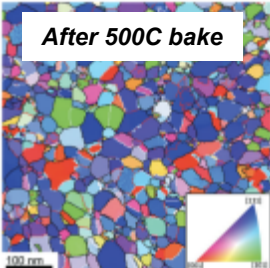
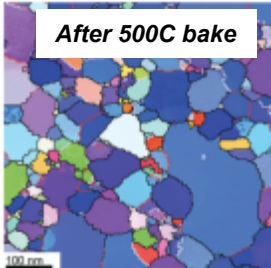
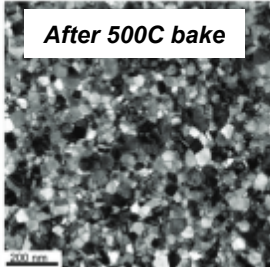
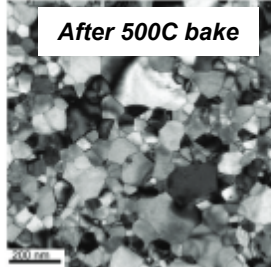
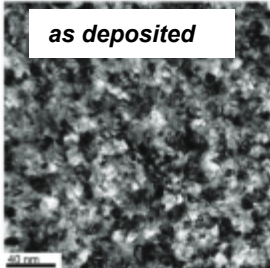
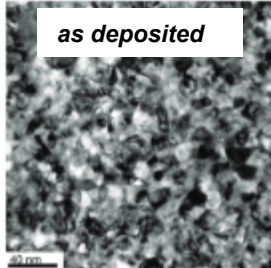
Interest in these stabilized alloys stems from their potential use as conductive, metal contacts including sliding metal contacts.

Sputter deposited Pt-Au exhibits nanocrystalline stability and retains excellent mechanical properties.

Grain structure

Pt

Pt_{0.9}Au_{0.1}

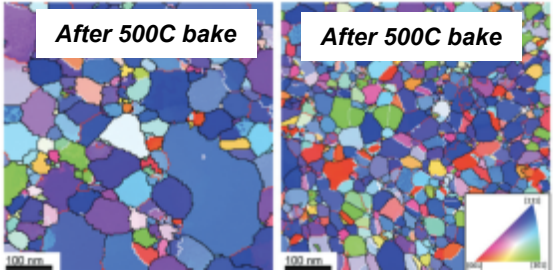
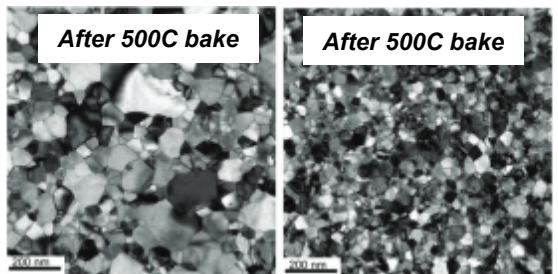
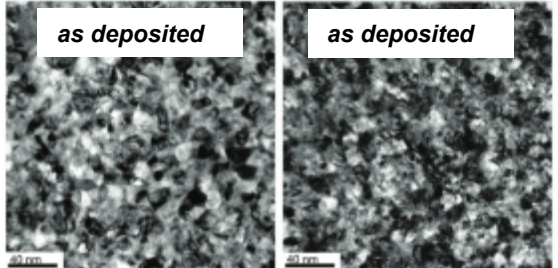


Sputter-deposited 9Pt/1Au
(Nanoscale, 2021 Bahr et al.)

Sputter deposited Pt-Au exhibits nanocrystalline stability and retains excellent mechanical properties.

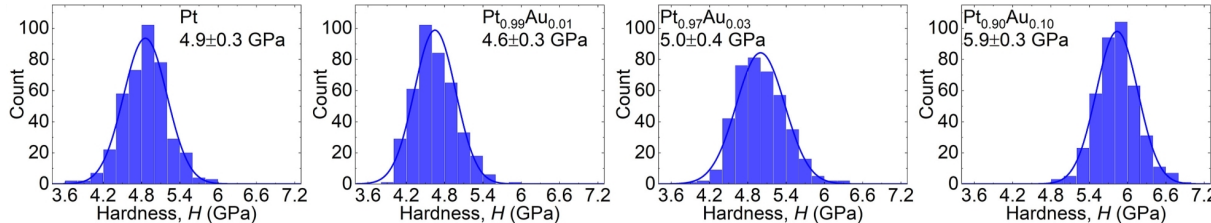
Grain structure

Pt Pt_{0.9}Au_{0.1}



Sputter-deposited 9Pt/1Au
(Nanoscale, 2021 Bahr et al.)

Hardness



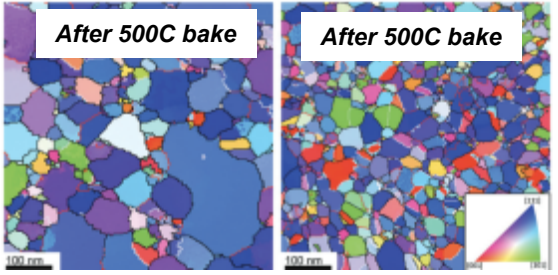
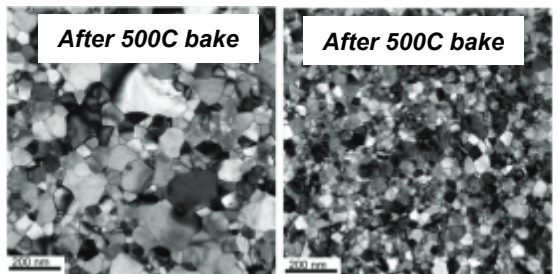
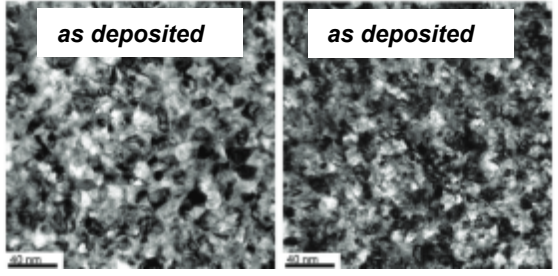
Hardness increases with Au addition up to 10 mol.% Au (Wear, 2023 DeIRio et al.)

Grain boundary segregation provides an alternative approach to improving mechanical response (different than solute strengthening, Zener pinning) for applications such as electrical contacts.

Sputter deposited Pt-Au exhibits nanocrystalline stability and retains excellent mechanical properties.

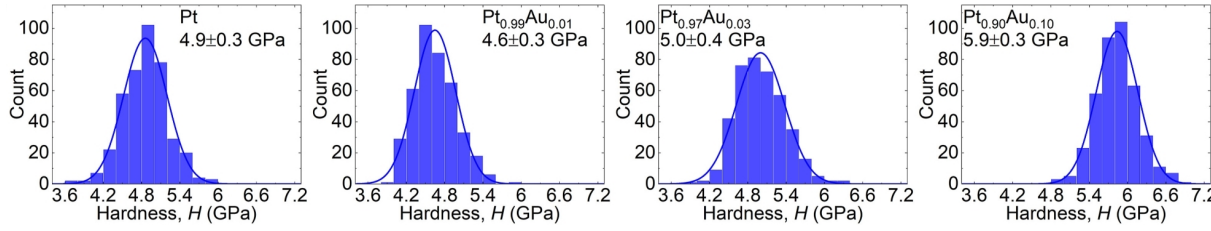
Grain structure

Pt Pt_{0.9}Au_{0.1}



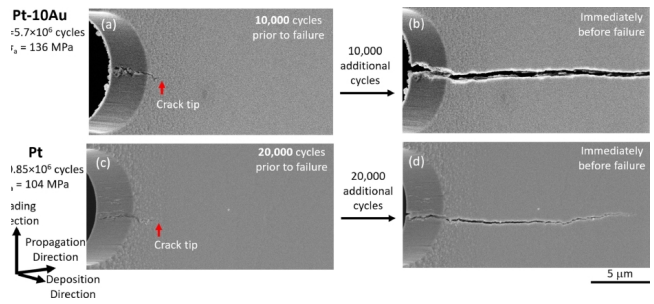
Sputter-deposited Pt_{0.9}Au_{0.1} (Nanoscale, 2021 Bahr et al.)

Hardness



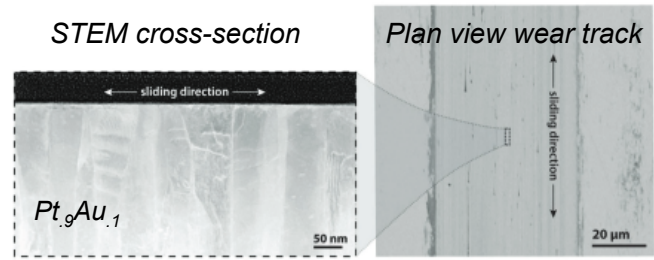
Hardness increases with Au addition up to 10 mol.% Au (Wear, 2023 DeIRio et al.)

Fatigue resistance



75% elevation of the fatigue endurance limit (Acta Mater., 2022 Heckman et al.)

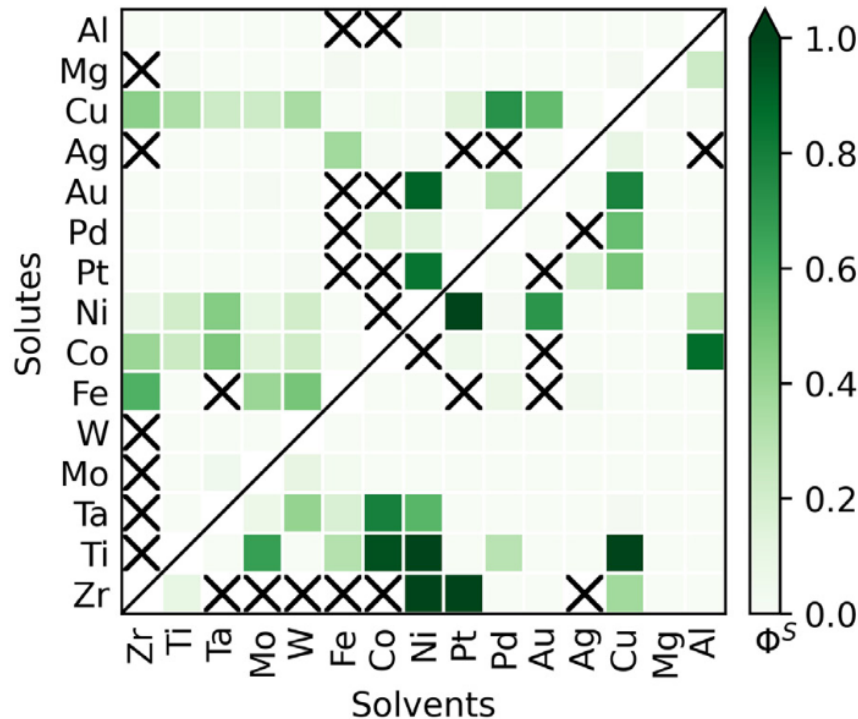
Wear



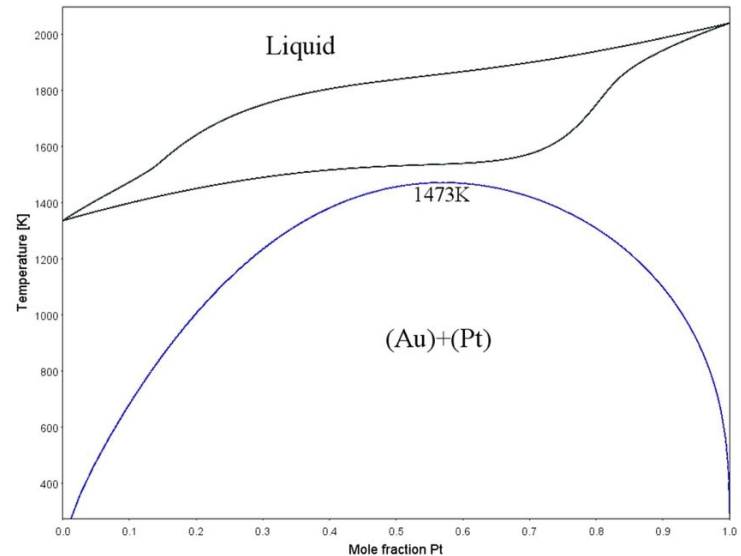
Friction coeff. ~ 0.01 & spec. wear rate ~ 10⁻⁹ mm³ N⁻¹ m⁻¹ attributed to C tribofilm (Adv. Materials, 2018 Curry et al.)

Grain boundary segregation provides an alternative approach to improving mechanical response (different than solute strengthening, Zener pinning) for applications such as electrical contacts.

Our team seeks to discover new, improved nanocrystalline, stable thin film materials for applications but is faced with a wealth of material choices.



The ground state stability score for the surveyed 210 alloys – ab initio study (Wagih and Schuh, PRL 2022).



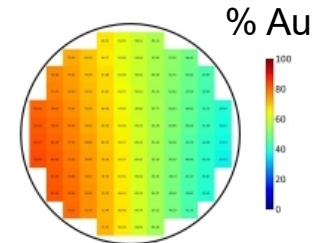
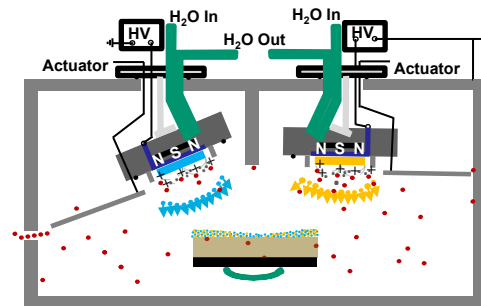
Pt-Au phase diagram (Hu, Xie et al., Mat. Res. Express 2022).

A vast number of binary systems are predicted to be stable but not vetted experimentally. However, the optimal compositions are not known.

Approach: combine high-throughput synthesis, rapid characterization & advanced analytical methods to expedite discovery.

Combinatorial deposition for fabricating 100s of different films in one experiment.

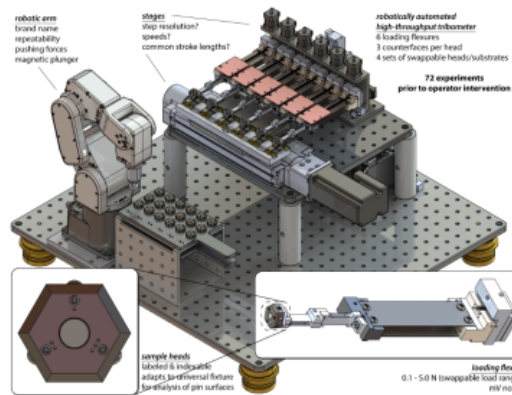
Confocal sputter deposition
Guided by Mod./Sim. for efficient DOEx



Combinatorial deposition on to fixed substrate creates graded composition

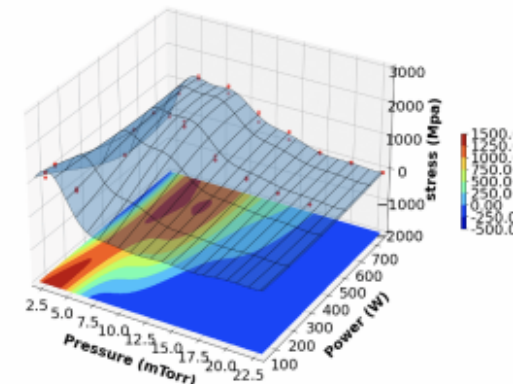
High-throughput characterization of properties, structure, etc.

Automated XRD, XRR, WDS, etc.
Expedited analysis when possible

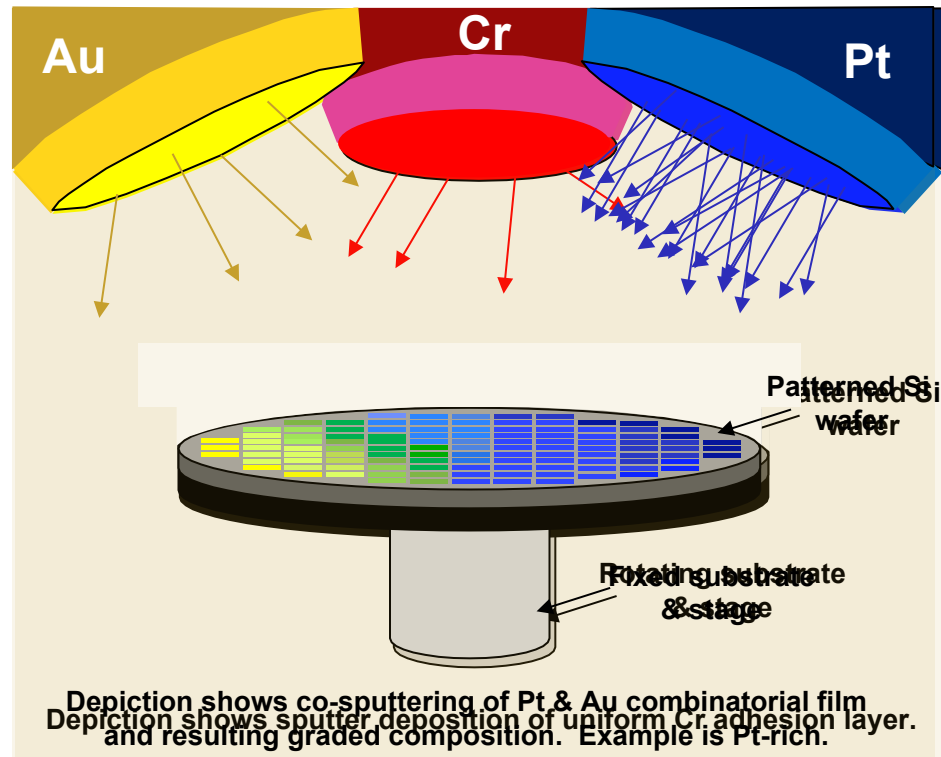


Machine Learning for correlation, optimization. Multi-dimensional.

Cluster analysis
Bayesian methods for optimization



Our combinatorial deposition approach utilizes multiple sputter targets (one element per gun) and masked substrate.



Step 2

All depositions involve pulsed DC magnetron sputtering in a Kurt J. Lesker PVD 200 system. The mask is patterned photoresist (removed after deposition).

We use a kinematic Monte Carlo program (SIMTRA) to efficiently guide multi-parameter depositions

SIMTRA inputs:

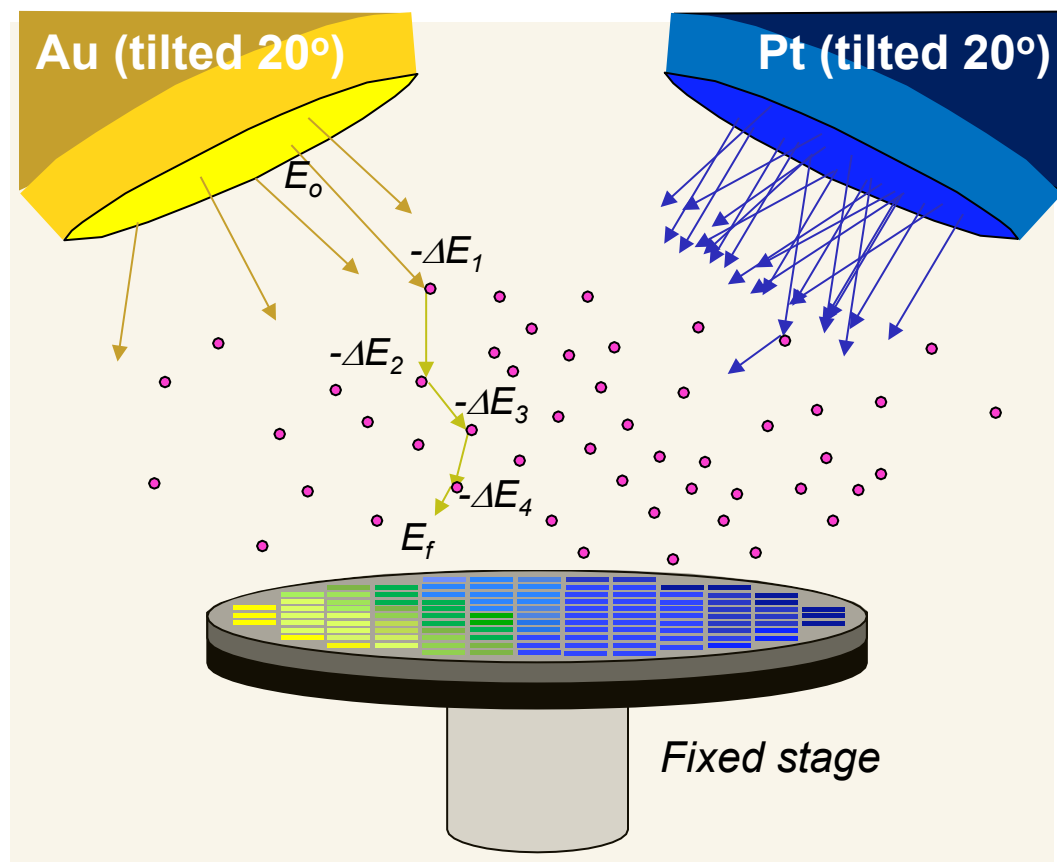
- Chamber and target geometry
- Ar ion spatial distribution on target
- Surface binding energy of target material
- Global angular distribution of ejecta from target
- Interaction potential (Moliere screen Coulomb)

SIMTRA execution:

- Tracks millions of sputtered metal atoms
- Accounts for the angle- and kinetic energy-changing collisions with rarefied Ar (10 mTorr)

SIMTRA outputs (for each metal target):

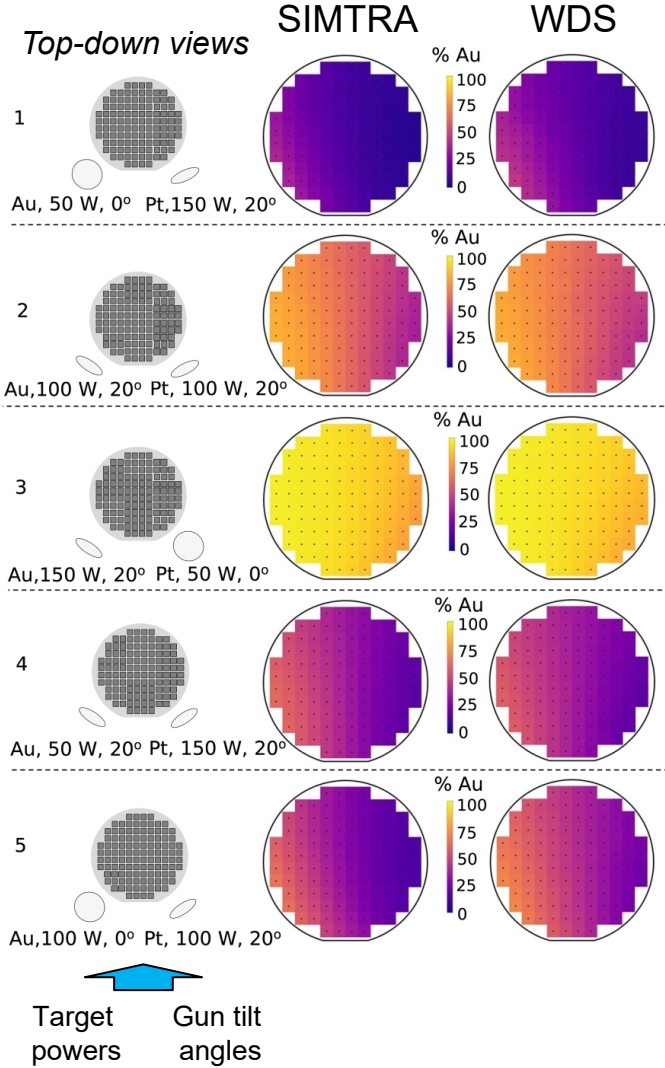
- Kinetic energy
- Incidence angle
- Landing location



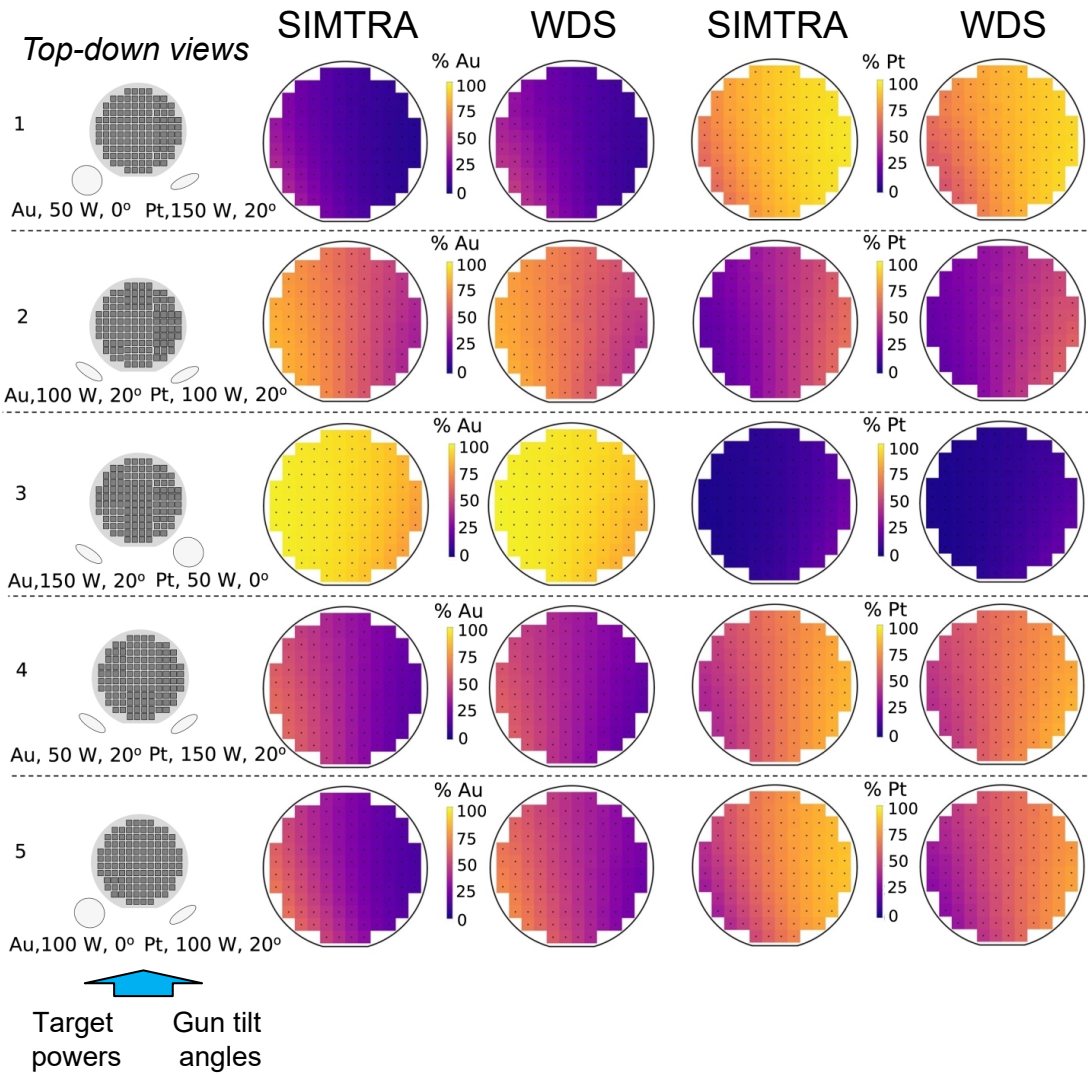
These produced results are binned to establish energy and angle distributions for each of the 112 areas on a combinatorial wafer.

Our team included $1e6$ metal atoms (per target) in each simulation. Simulations of each deposition experiment were repeated 20 times for good statistics.

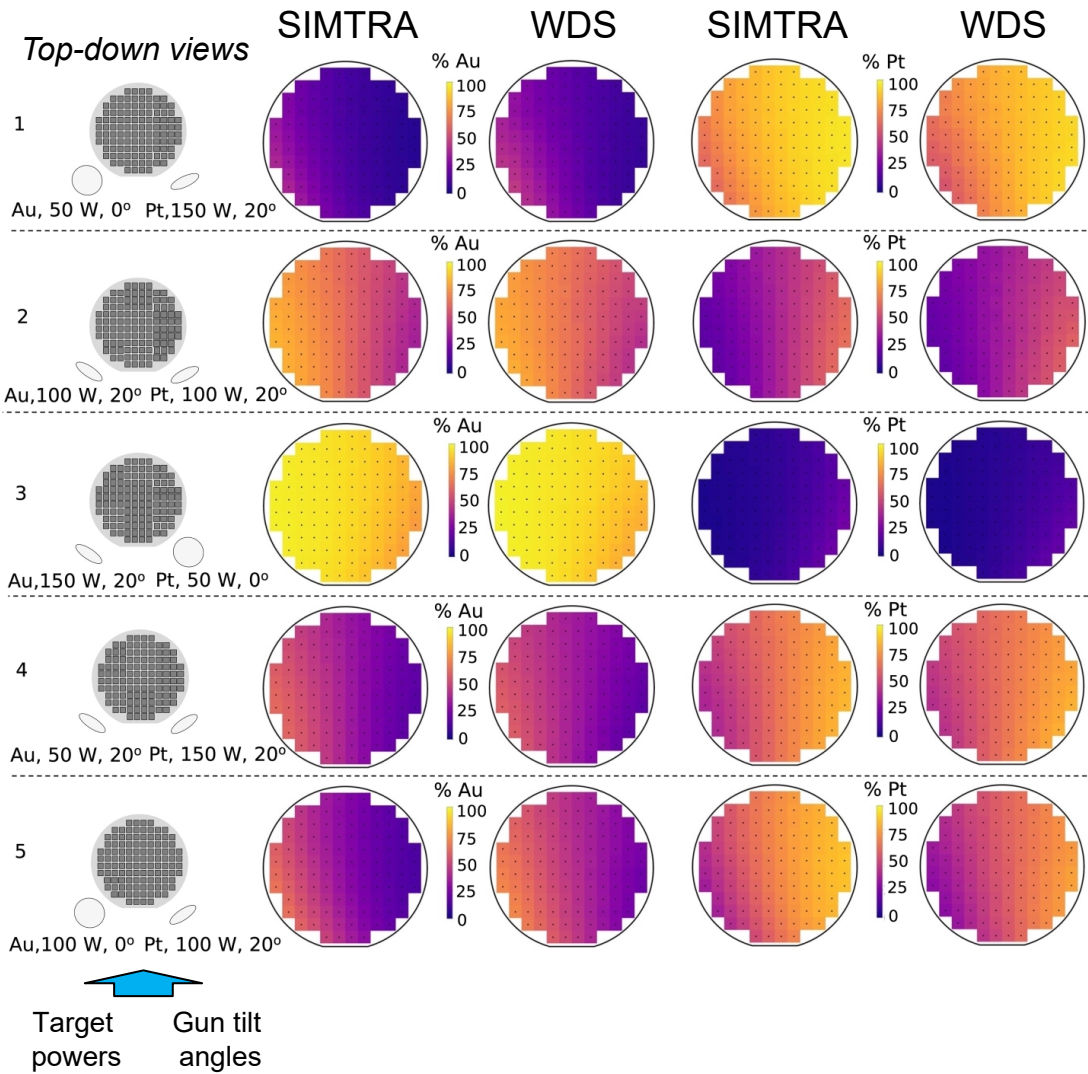
SIMTRA-predicted compositions closely match values measured by Wavelength Dispersive Spectroscopy (WDS).



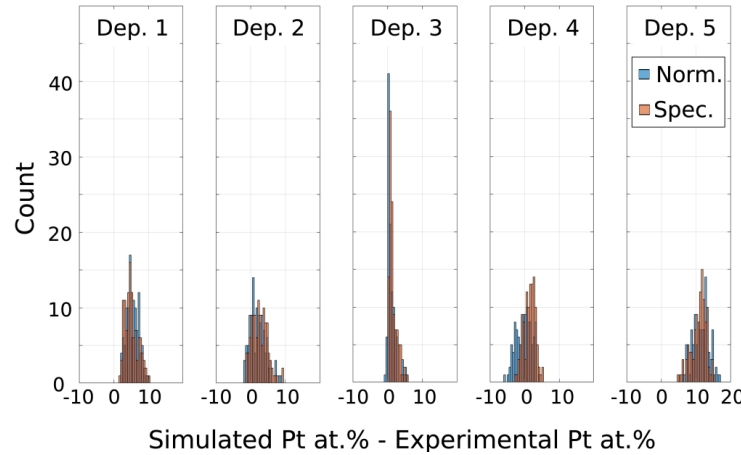
SIMTRA-predicted compositions closely match values measured by Wavelength Dispersive Spectroscopy (WDS).



SIMTRA-predicted compositions closely match values measured by Wavelength Dispersive Spectroscopy (WDS).

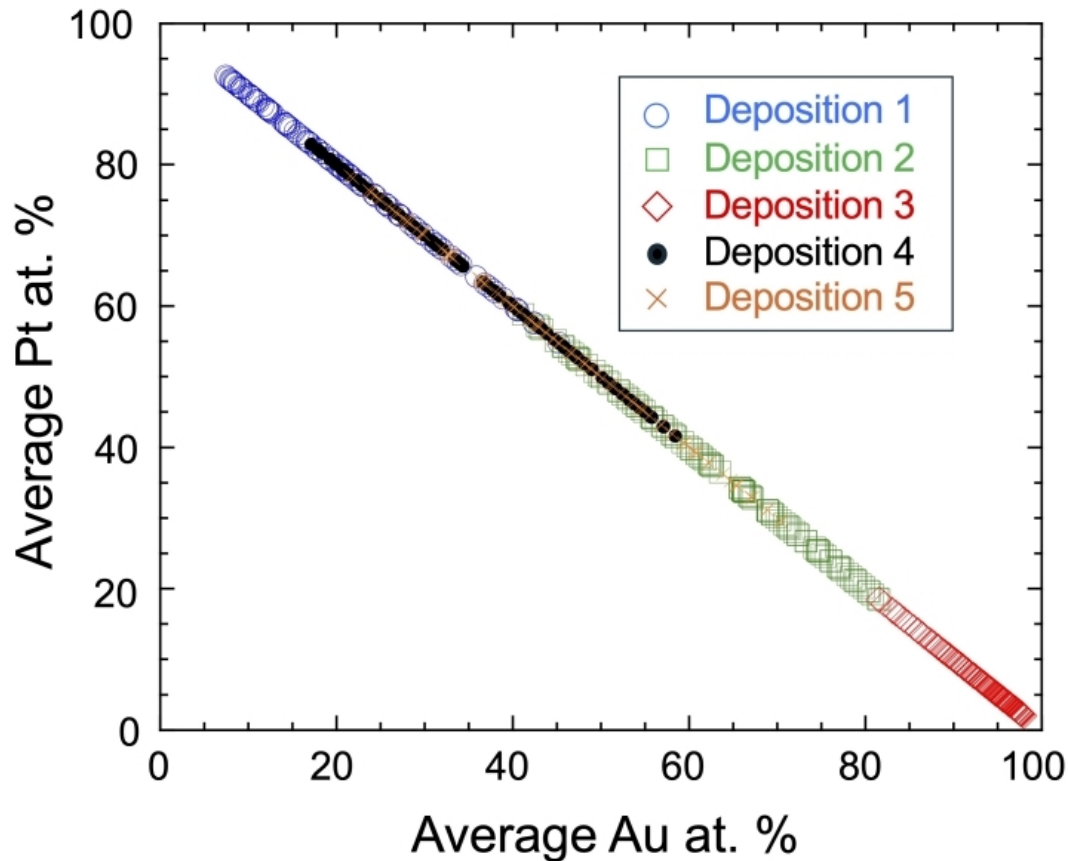


Detailed comparisons show Agreement with 5% in most cases



The excellent matching of predicted vs. experimental compositions has led us to adopt SIMTRA for guiding additional combinatorial depositions (CuAg, NiPt).

SIMTRA-guided depositions achieved our goal to attain a broad range of composition.



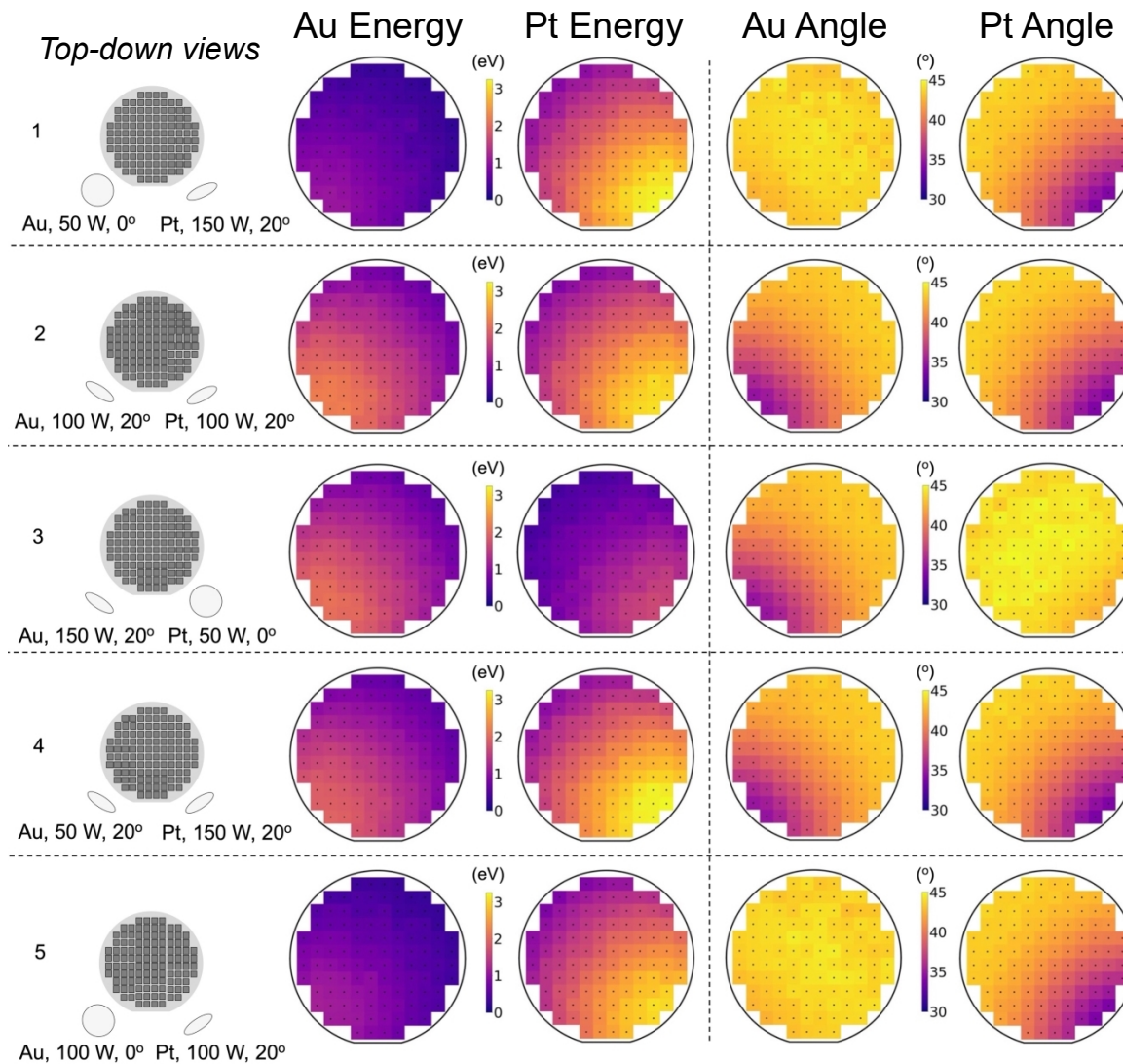
Three depositions (#1-3) spanned nearly full range.

Small increments provided.

No large gaps in composition.

Additional depositions (#4, 5) overlapped composition ranges but provided access to different kinetic energies and incidence angles.

Additional SIMTRA outputs include incident atom kinetic energy and angle of incidence distributions.

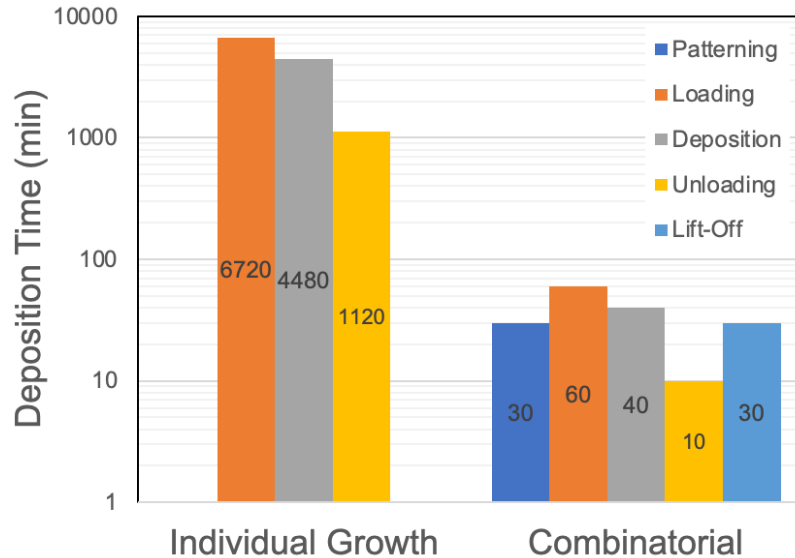


Average values obtained from predicted distributions are shown in maps.

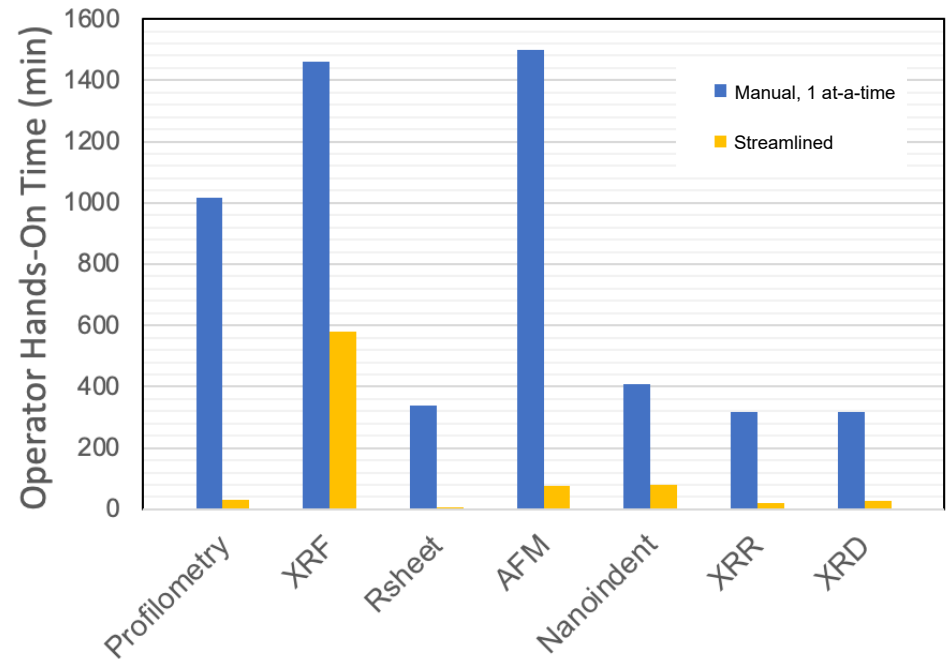
Higher kinetic energy in areas lying closer to associated target due to reduced number of collisions with Ar.

These average values and other moments of distributions were used in analysis.

The gains associated with combinatorial deposition have been coupled with streamlined characterization.



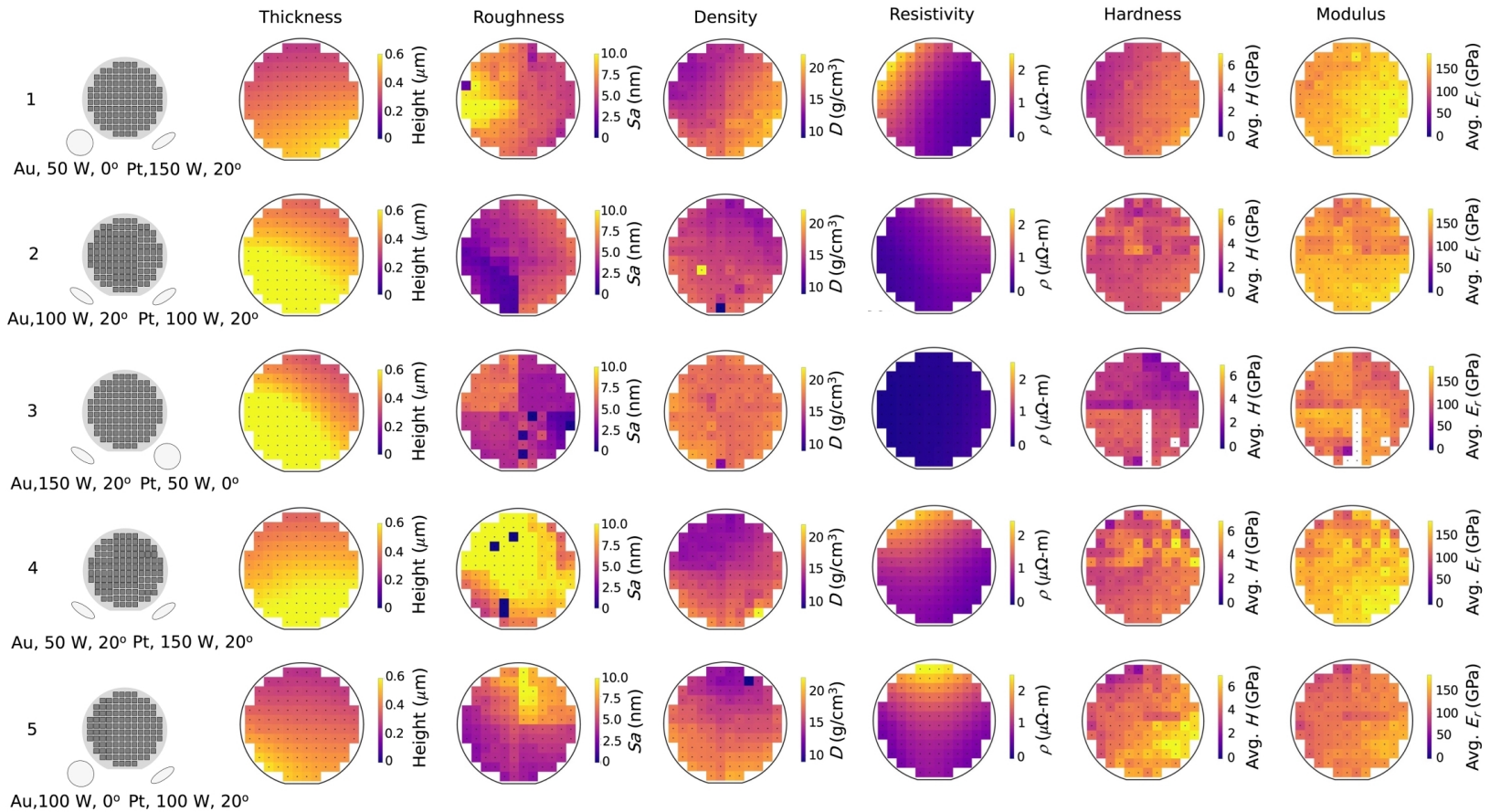
Gains are attributed to automated instruments and some improved analysis techniques (such as fast X-ray reflectivity)



Approximately 1e3– 1e4 data sets acquired in 1 month using improved methods.

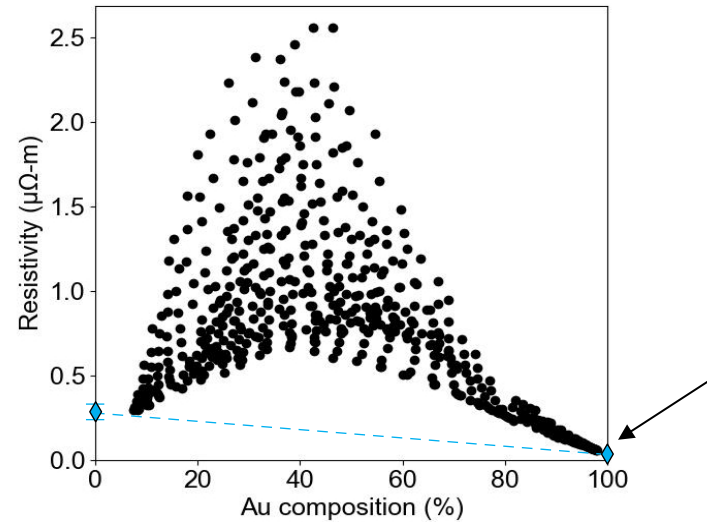
Streamlined characterization has generated 11 modalities

– often expressed with scalar value maps

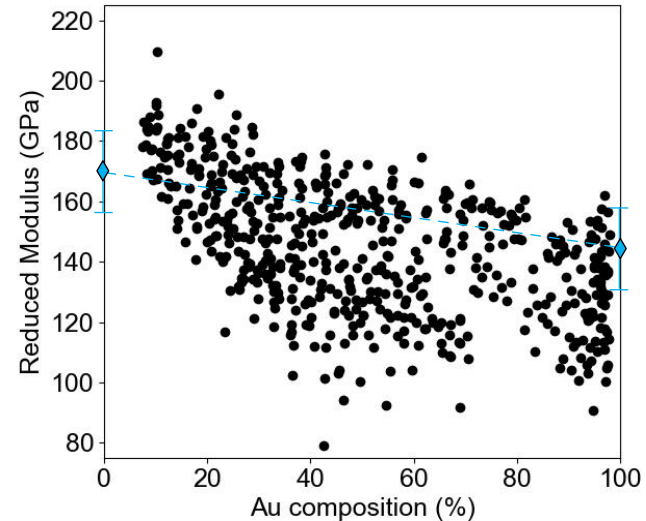
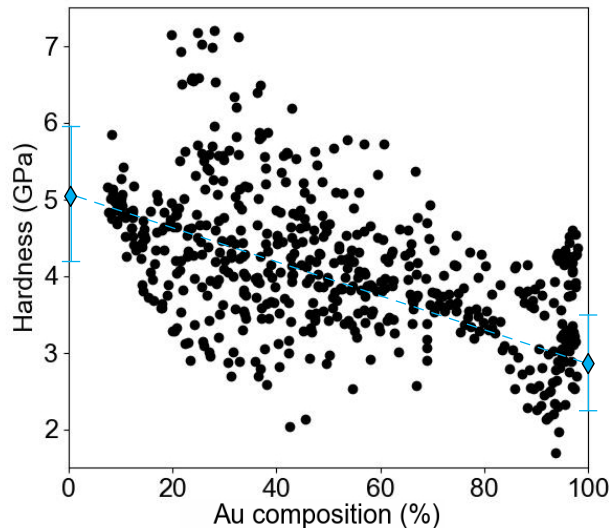


In addition, several scalar signatures derive from XRD. This includes (111) and (200) peak widths, relative intensities (I_{111}/I_{200}), and 2θ peak positions.

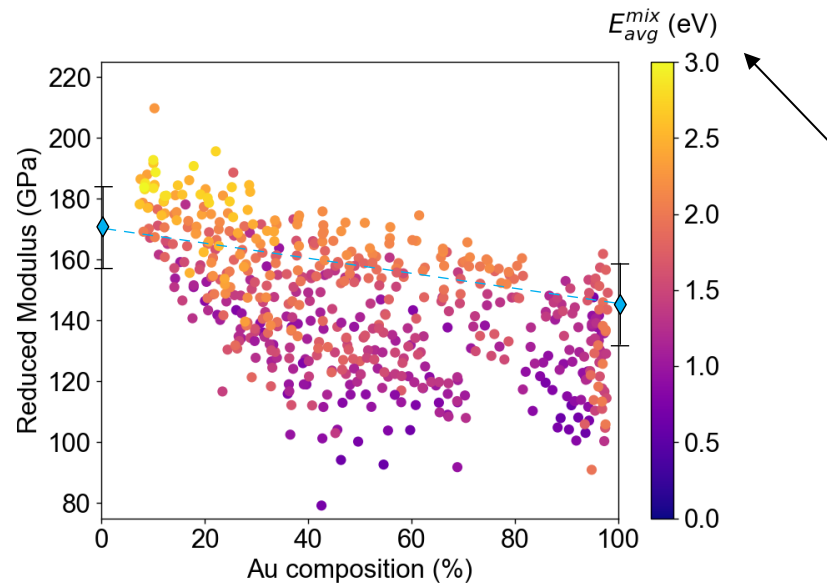
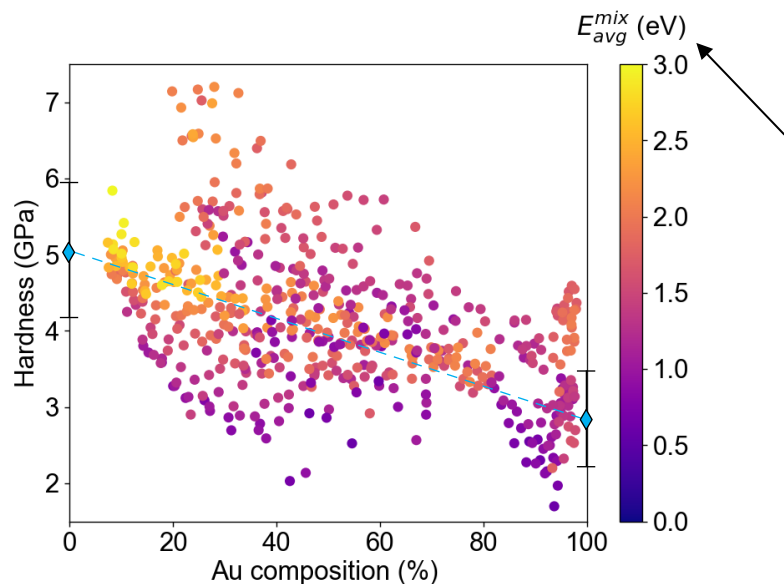
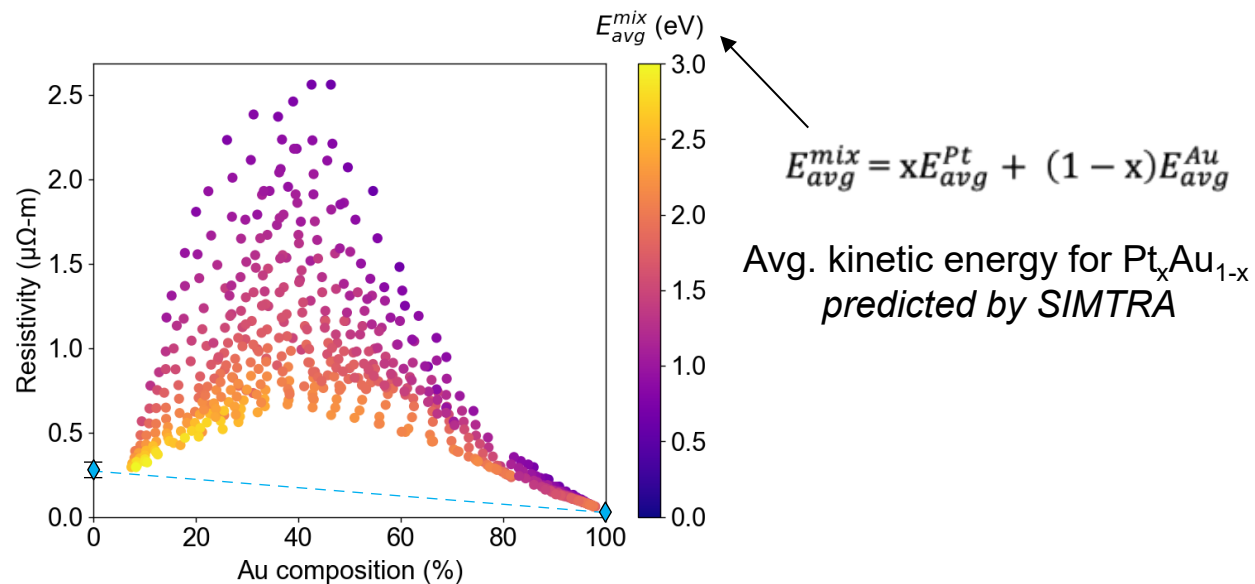
Resistivity, hardness and modulus determined using automated nanoindentation and 4-point probe testing.



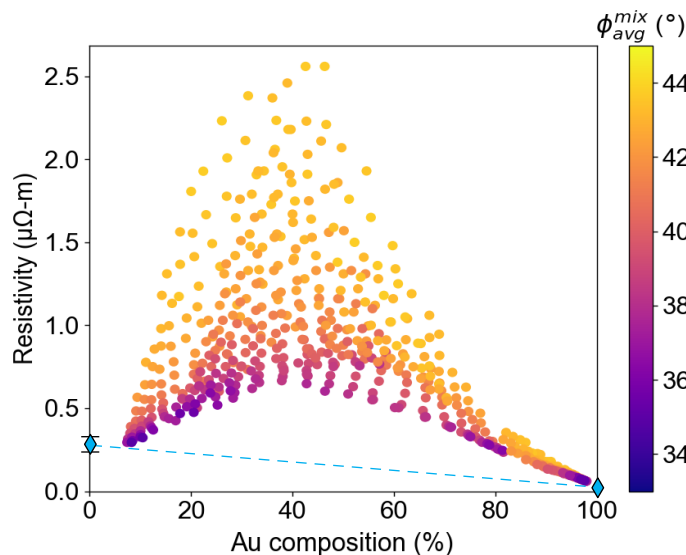
Dashed, straight line is drawn based solely on measured results for pure Pt and pure Al films shown with single diamond symbols. The dashed line is not a fit to the combi Pt-Au film data.



Three key modalities evaluated across full range of composition in terms of deposition energy.

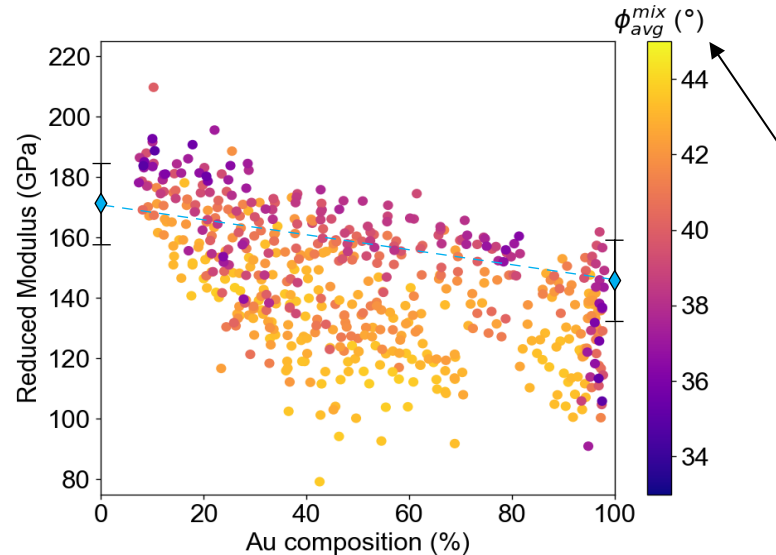
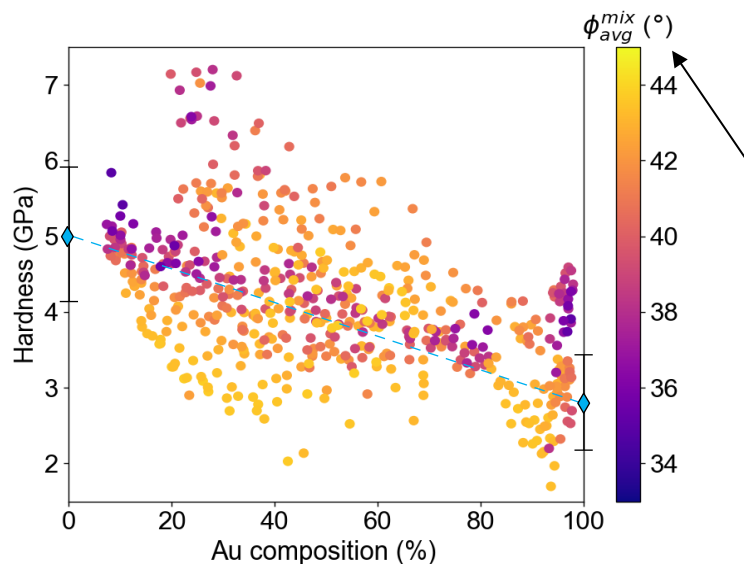


Three key modalities evaluated across full range of composition in terms of incidence angle.

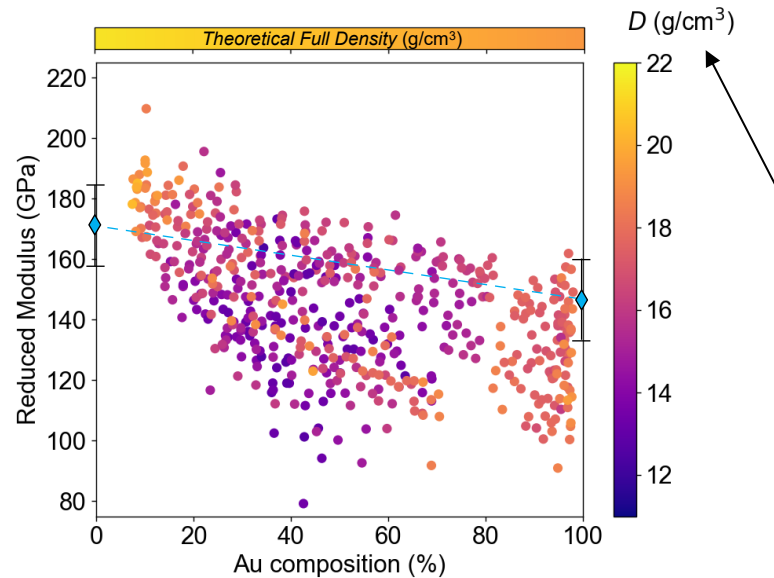
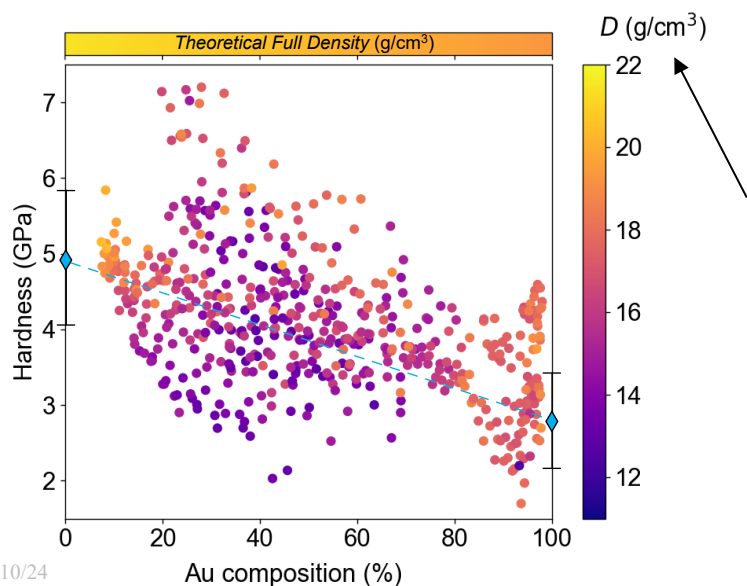
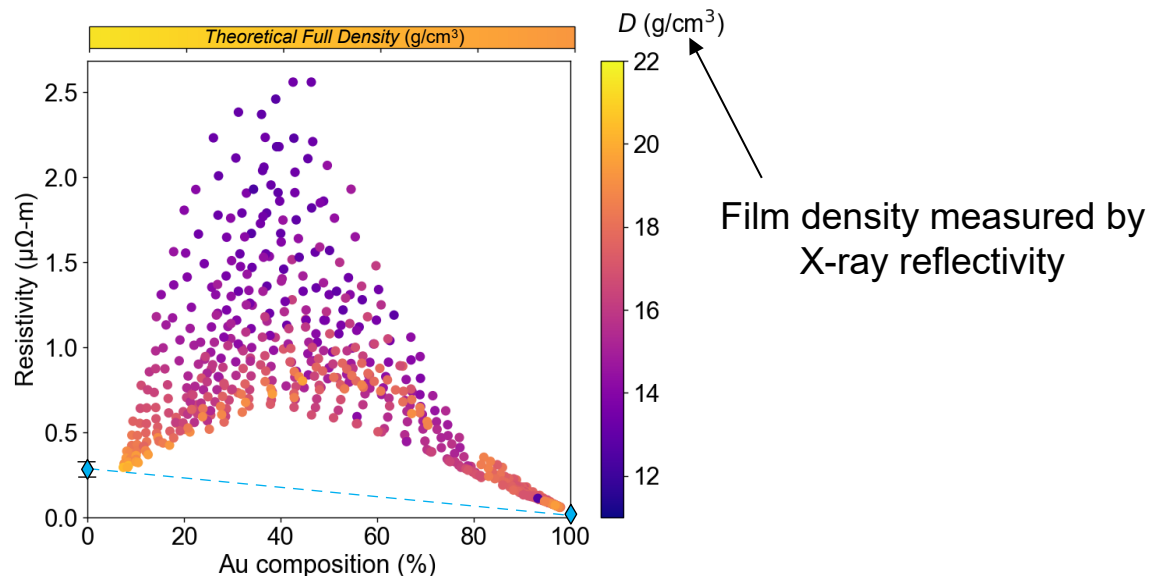


$$\phi_{avg}^{mix} = x\phi_{avg}^{Pt} + (1-x)\phi_{avg}^{Au}$$

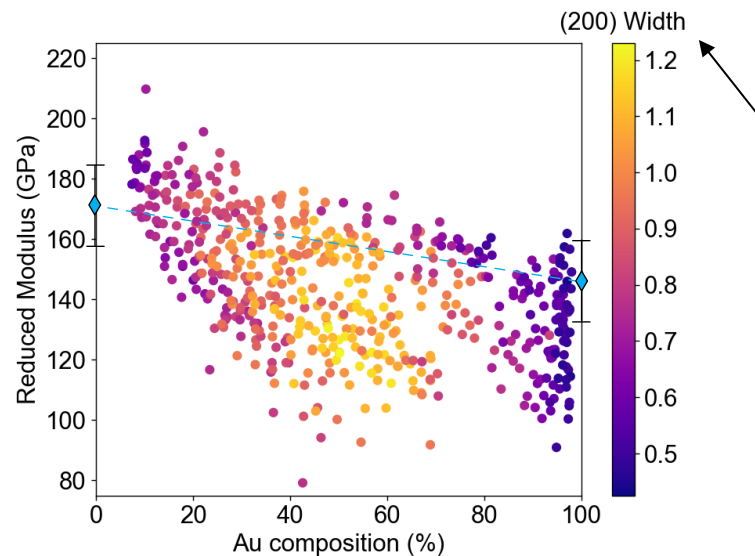
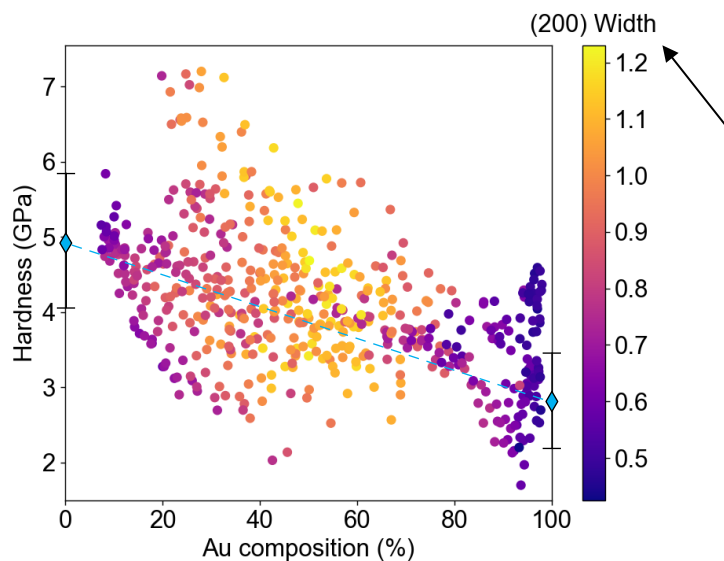
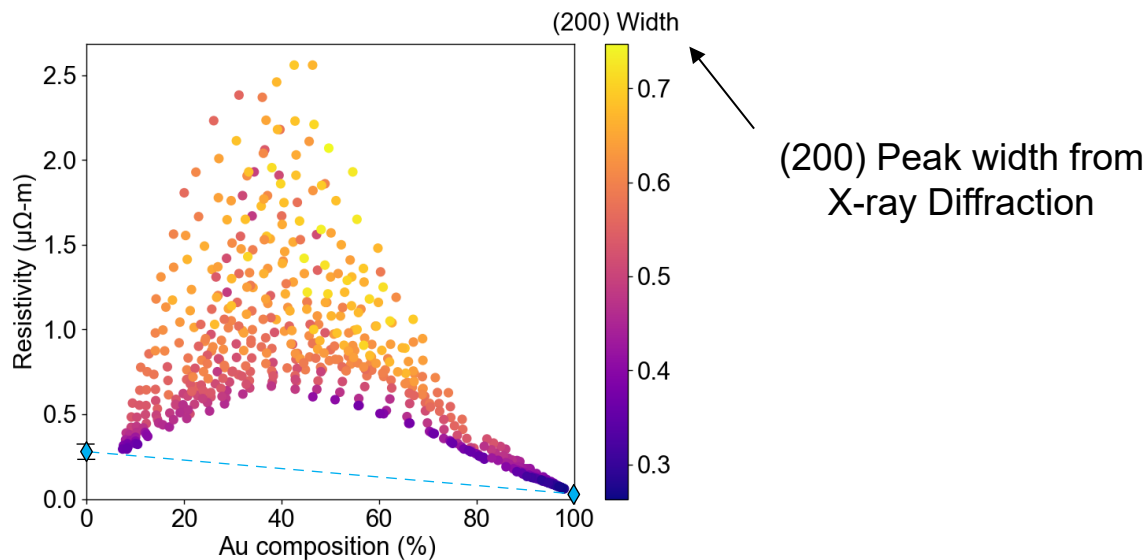
Avg. incidence angle for $\text{Pt}_x\text{Au}_{1-x}$
predicted by SIMTRA



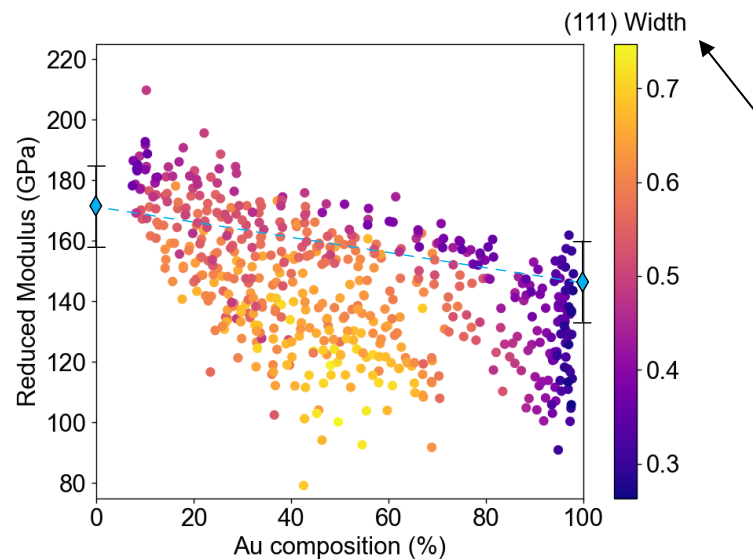
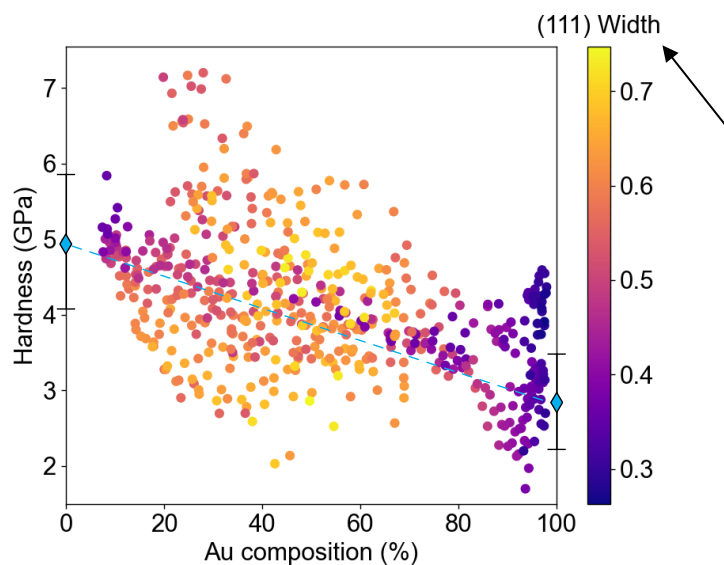
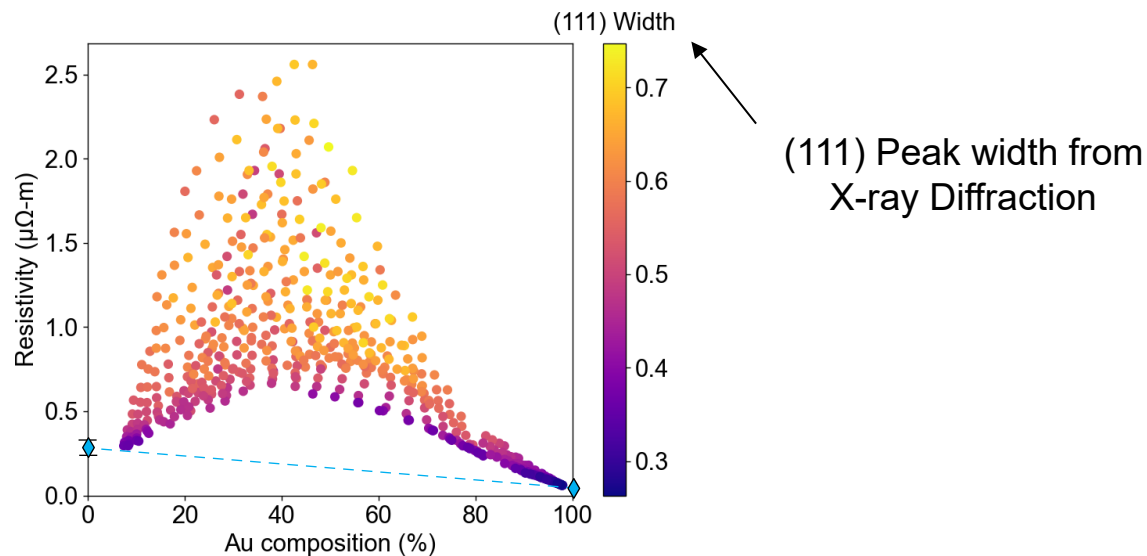
Three key modalities evaluated across full range of composition in terms of density.



Three key modalities evaluated across full range of composition in terms of XRD peak widths.

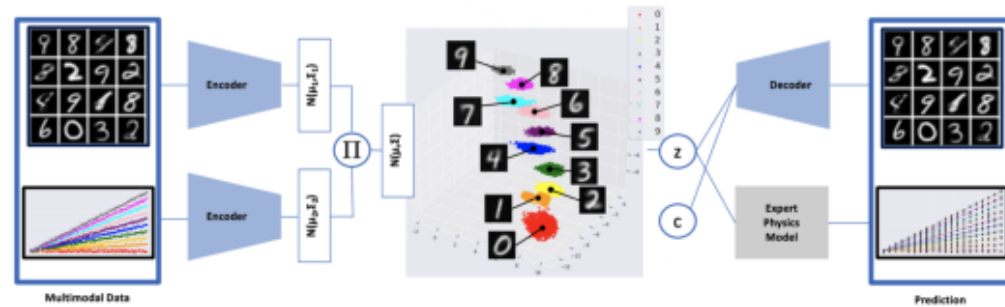


Three key modalities evaluated across full range of composition in terms of XRD peak widths.



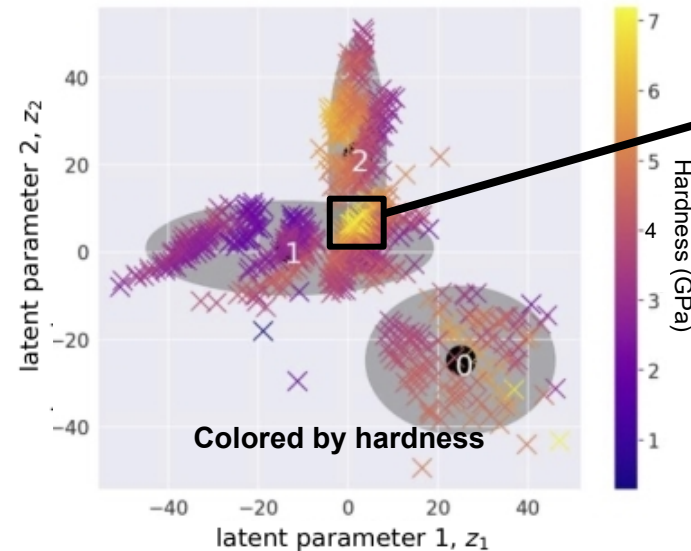
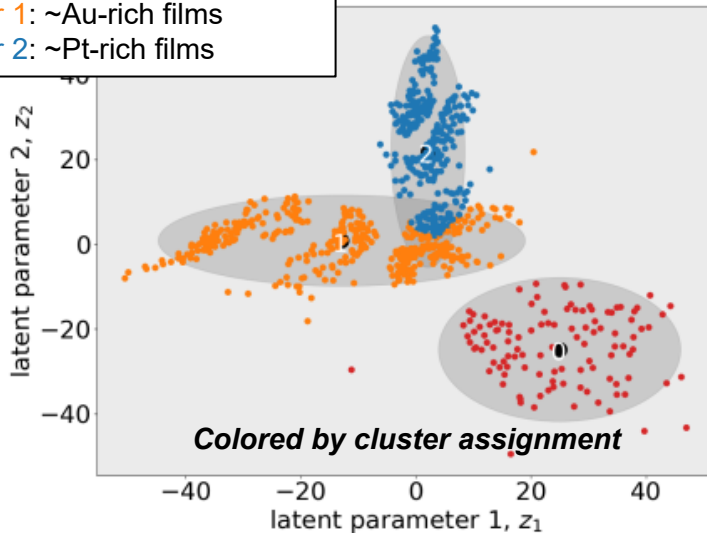
Additional investigations of exemplar Pt_x-Au_{1-x} films have implemented machine learning methods (PIMA).

Approach: Physics-Informed Multimodal Autoencoder (PIMA)



Walker et al. 2024, Foundations of Data Science; doi:10.3934/fods.2024019

Cluster 0: 20-60% Au films
Cluster 1: ~Au-rich films
Cluster 2: ~Pt-rich films



Majority of high-hardness films lie in this region

Turn to Pearson correlations for identifying potential ties to process & structure.

Clustering of the data has enhanced interpretability beyond original analysis

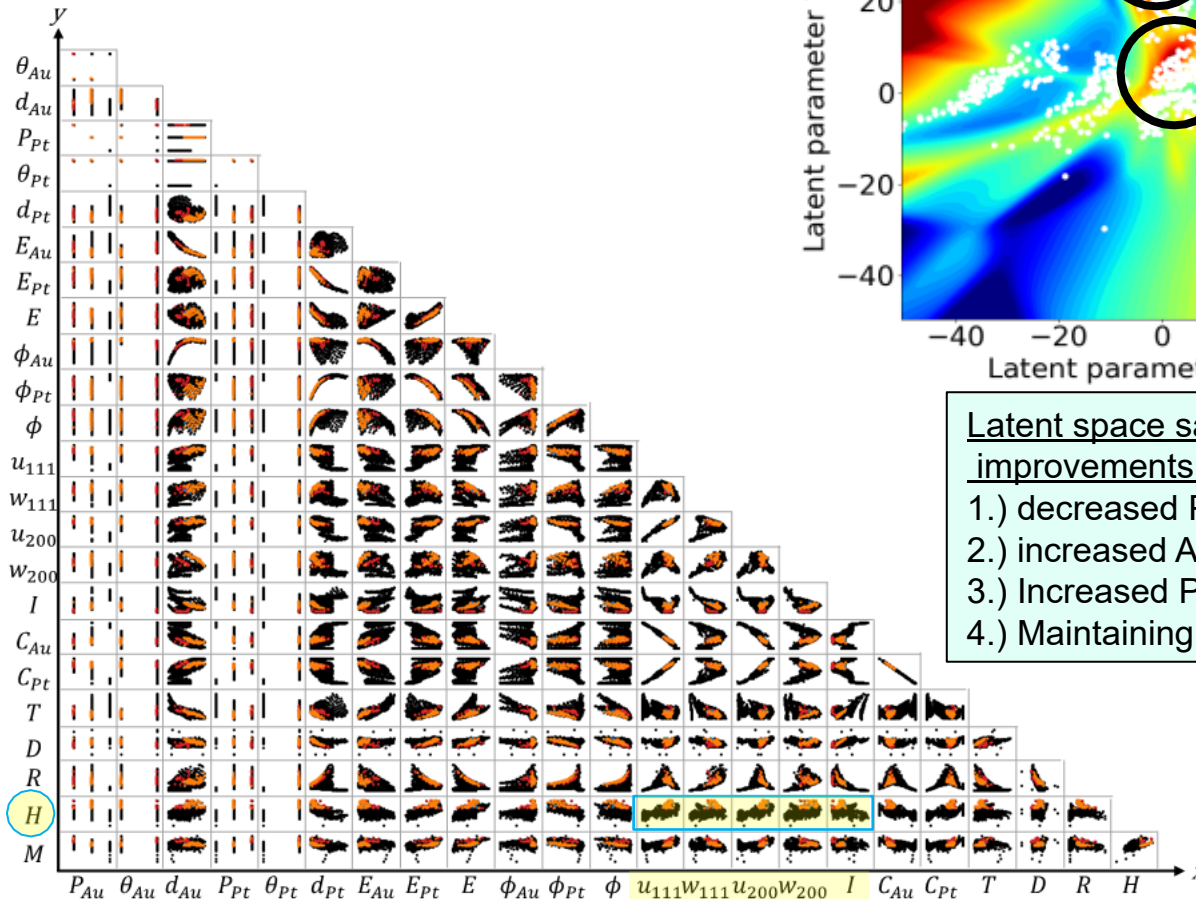
Pair wise correlation plots

Data filtered for 15 to 45% Au, Hardness > 5

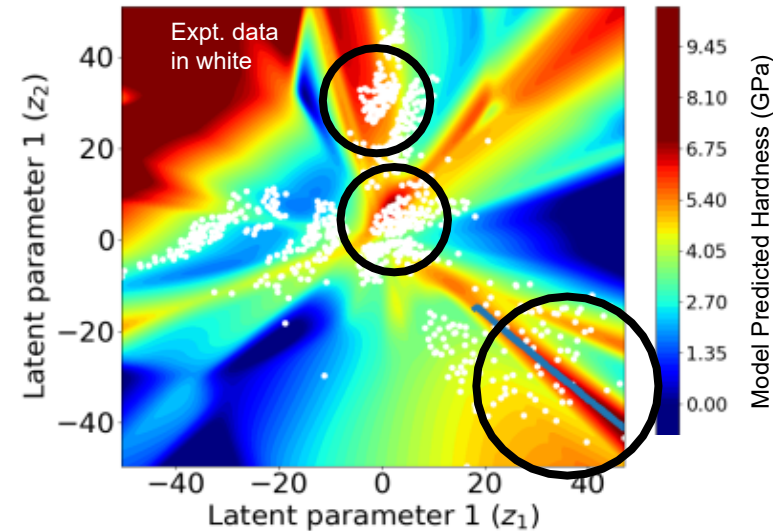
Detailed evaluation of pairwise evaluations points to strong correlations with XRD peak position (u_{111} , u_{200}), peak widths (w_{111} , w_{200}) and rel. peak intensities (I).

Nomenclature

P_{Au} = Au gun power
 θ_{Au} = Au gun angle
 d_{Au} = Au gun distance
 P_{Pt} = Pt gun power
 θ_{Pt} = Pt gun angle
 d_{Pt} = Pt gun distance
 E_{Au} = Au average energy
 E_{Pt} = Pt average energy
 E = Average energy
 ϕ_{Au} = Au average angle
 ϕ_{Pt} = Pt average angle
 ϕ = Average angle
 u_{111} = XRD peak 111 loc.
 w_{111} = XRD peak 111 width
 u_{200} = XRD peak 200 loc
 w_{200} = XRD peak 200 width
 I = log10 Intensity ratio
 C_{Au} = Au composition
 C_{Pt} = Pt composition
 T = Thickness
 D = Density
 R = Resistivity
 H = Hardness
 M = Modulus



3 regions (where data exists) that suggest regions of increasing hardness



Latent space sampling suggests improvements via:

- 1.) decreased Pt gun distance
- 2.) increased Au gun distance
- 3.) Increased Pt power
- 4.) Maintaining Pt gun angle

Summary

- Combinatorial deposition of Pt-Au films was successfully guided by a Kinematic Monte Carlo program (SIMTRA) to achieve an intended, broad range of film composition w/ fine increments in relatively few depositions.
- High throughput, automated methods and improved analysis techniques have enabled measurement of 11 modalities of all produced films in reasonable time. (means $1e3$ to $1e4$ data sets per month).
- Combinatorial Pt-Au films exhibited:
 - substantial variation in resistivity (ρ), hardness (H) and modulus (E_r)
 - ρ , H and E_r varied with atom kinetic energy, inc. angle and film density
 - large $H > 6 \text{ GPa}$ for a new range of compositions (20-40 mol.% Au)
- ML analysis revealed that the high hardness is positively correlated with
 - XRD peak positions (infer film stress)
 - XRD peak widths (possible Hall-Petch relation)
 - XRD peak intensity ratio (texture)
- Implemented machine learning method (PIMA) used to suggest improvements.

Acknowledgements

Experimental and machine-learning capabilities are supported in part by the Center for Integrated Nanotechnologies, an Office of Science user facility operated for the U.S. Department of Energy. This work was funded by the Laboratory Directed Research and Development program at Sandia National Laboratories.

EXTRA SLIDES

Hardness correlation coefficients

Nontrivial subsets of the data
unveil unique, cluster specific
correlations

Correlations with respect to all clusters
in agreement with those in *D.P. Adams
et al., Journal of Vacuum Science &
Technology A (2024)*

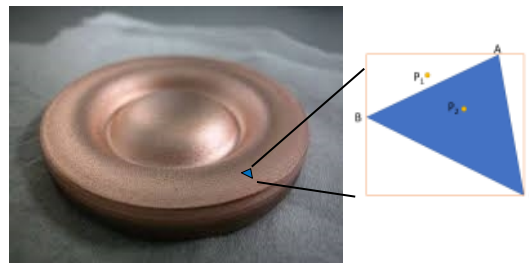
Modality	Cluster 0	Cluster 1	Cluster 2	All clusters
d_{Au}	0.309	-0.034	0.279	0.295
d_{Pt}	-0.406	-0.479	-0.736	-0.626
E_{Au}	-0.295	0.011	-0.176	-0.303
E_{Pt}	0.368	0.502	0.697	0.638
ϕ_{Au}	0.331	-0.017	0.221	0.224
ϕ_{Pt}	-0.338	-0.465	-0.699	-0.610
u_{111}	0.545	0.617	0.278	0.697
w_{111}	-0.215	0.511	-0.450	0.310
u_{200}	0.512	0.620	0.341	0.703
w_{200}	-0.313	0.553	-0.111	0.317
I	-0.296	-0.385	0.469	-0.407
C_{Au}	-0.557	-0.606	-0.201	-0.680
C_{Pt}	0.557	0.606	0.201	0.680
T	0.131	0.187	0.439	-0.040
D	0.017	-0.230	0.645	0.182
R	-0.190	0.412	-0.573	0.140
H	1.000	1.000	1.000	1.000
M	0.697	0.370	0.379	0.562

XRD features {
Composition {

Steps to estimating a global angular distribution (used in SIMTRA studies)

Steps follow the general methods of *Boydens et al.**

1.) measure target shape & roughness



Triangle tessellation wherein each $\sim 500 \mu\text{m}$ long mesh element has a well defined θ

2.) mesh surface (triangle tessellation)
- each triangle has well-defined normal

3.) interpret erode profile as = incident Ar ion distribution on target

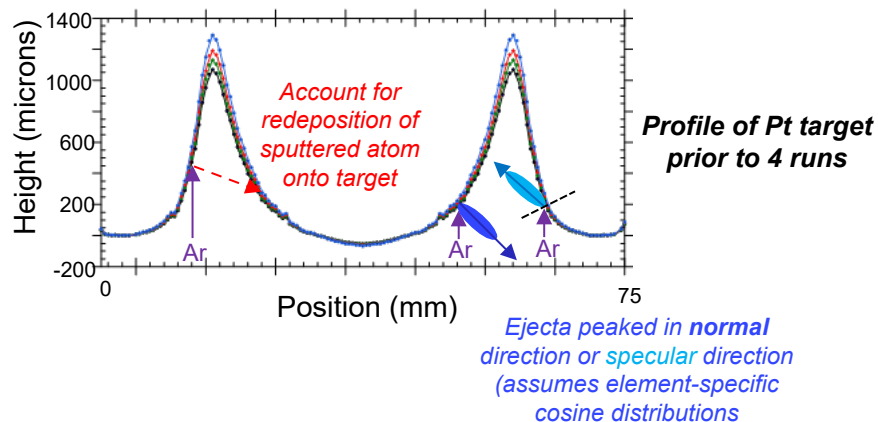
4.) estimate sputter yield angular dependence
- use Yamamura formulation for $Y(\theta)$
- $Y(0^\circ)$ from SRIM 2013

5.) account for **re-deposition** of sputtered metal atoms
- assume sticking coefficient = 1

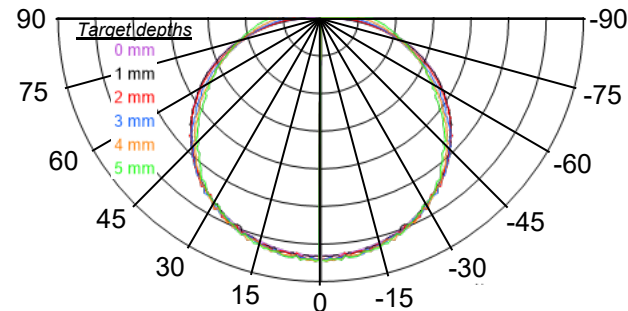
6.) utilize published **ejecta spatial profiles** and apply to each mesh element defined by its angle
- two cases considered as shown

7.) integrate over all mesh elements comprising target

8.) scale total emitted metal atom flux according to measured Ar ion currents incident on targets



Output: global angular distributions of sputter-emitted metal atoms for different target depths (example is Pt)

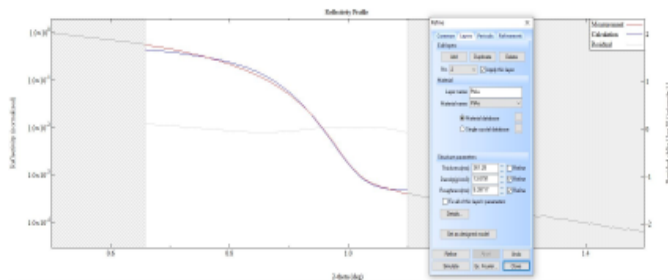
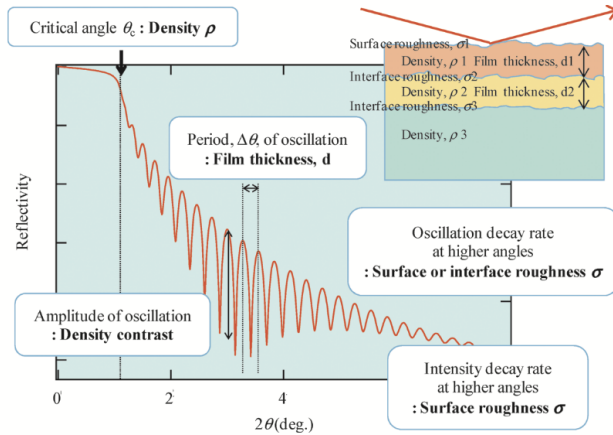


* Boydens et al. Thin Solid Films (2013)

Fast X-ray reflectivity for thin film density determination of combinatorial films.

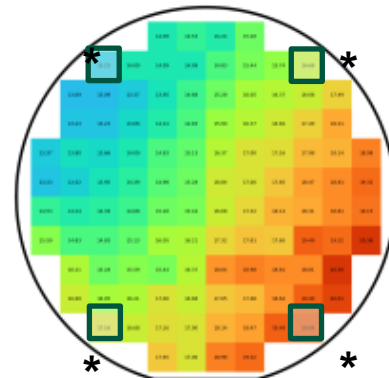
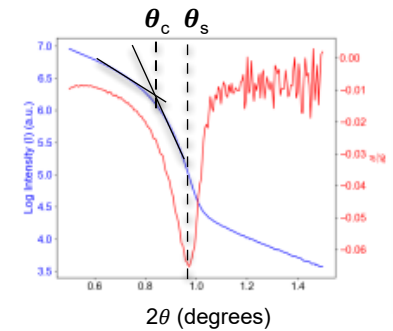
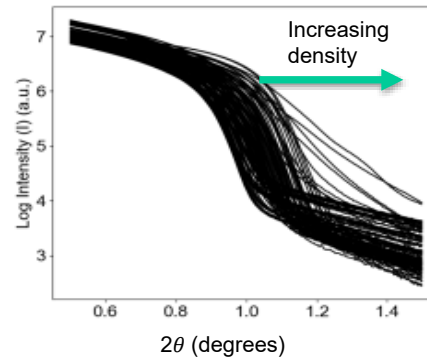
Traditional Method

- High resolution optics ARE required
- Seeks Density, Thickness, Roughness x2
- GlobalFit applied to all areas of interest

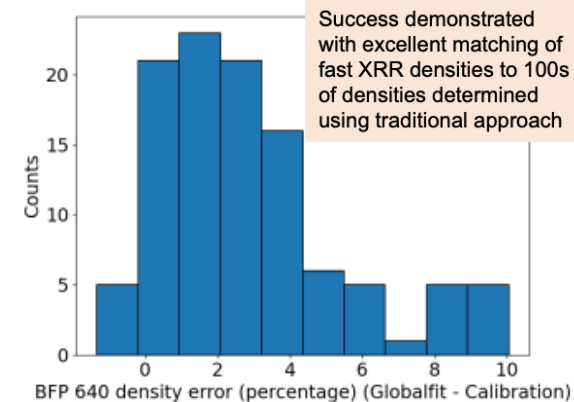


Our New Streamlined Method

- ONLY determining density → high resolution optics NOT required
- Use x-y stage for unattended translation, continued acquisition
- First derivative method to identify θ_s = streamlined critical angle
- Because θ_s is consistently $> \theta_c$ calibrate by measuring a handful of anchors
- Apply offset from anchors to full wafer

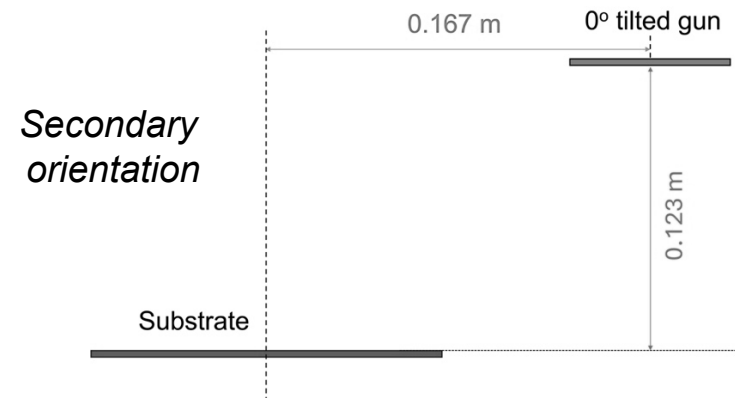
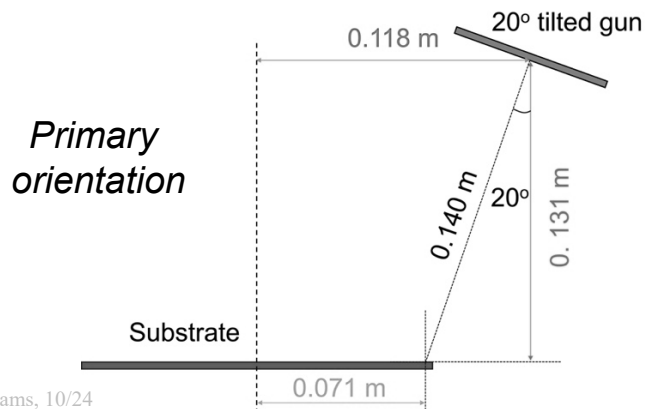


* anchors

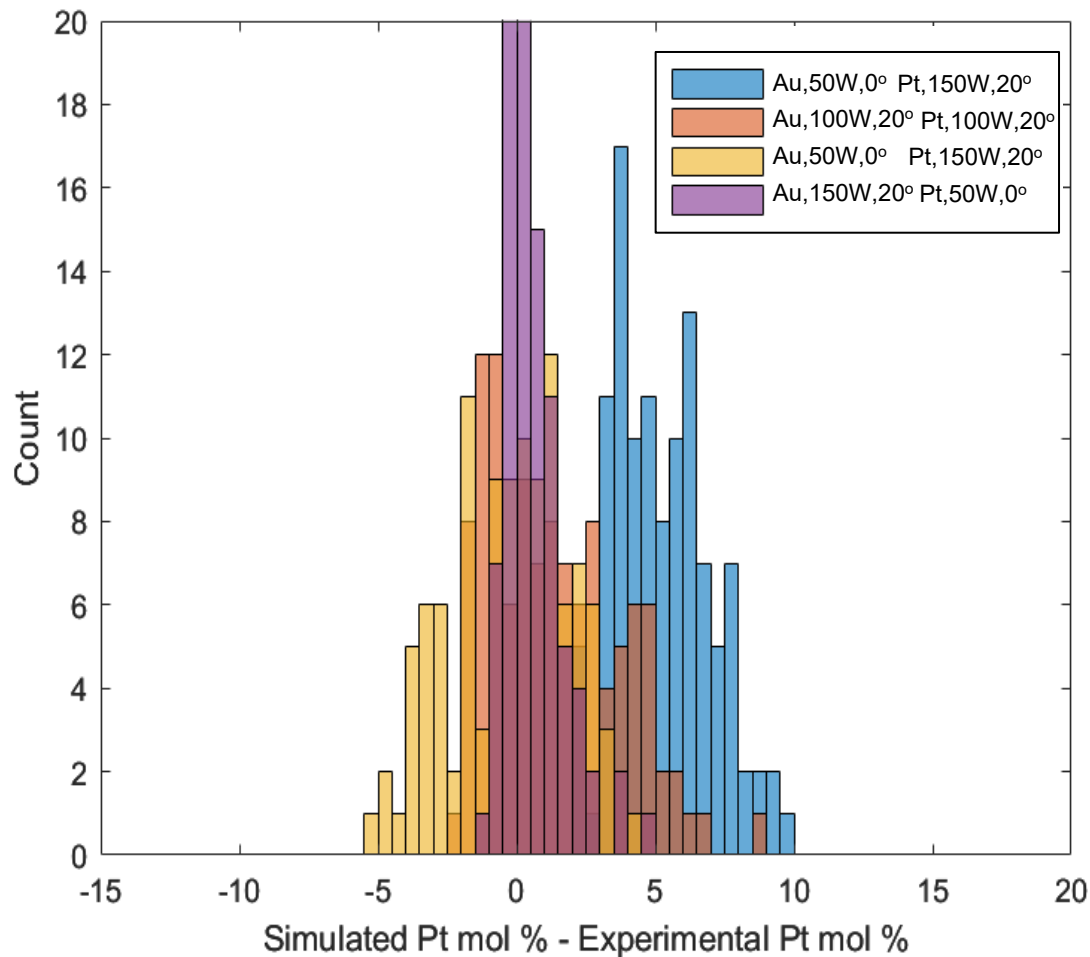


Summary of deposition conditions used in combinatorial Pt-Au study (including single element depositions)

Deposition/ Sample ID	Pt gun angle, °	Au gun angle, °	Pt gun power, W	Au gun power, W	Pt gun V_d , V	Au gun V_d , V
1	20	0	150	50	444 (5.3)	317 (6.1)
2	20	20	100	100	418 (5.1)	379 (7.6)
3	0	20	50	150	370 (5.1)	357 (7.1)
4	20	20	150	50	448 (6.6)	317 (7.1)
5	20	0	100	100	413 (7.0)	354 (4.5)
Pure Pt	20	n/a	100	n/a	417 (0.7)	n/a
Pure Au	n/a	20	n/a	100	n/a	391 (0.2)



Comparisons across multiple depositions show that SIMTRA-predicted compositions are within a few mol.% of WDS-measured values.



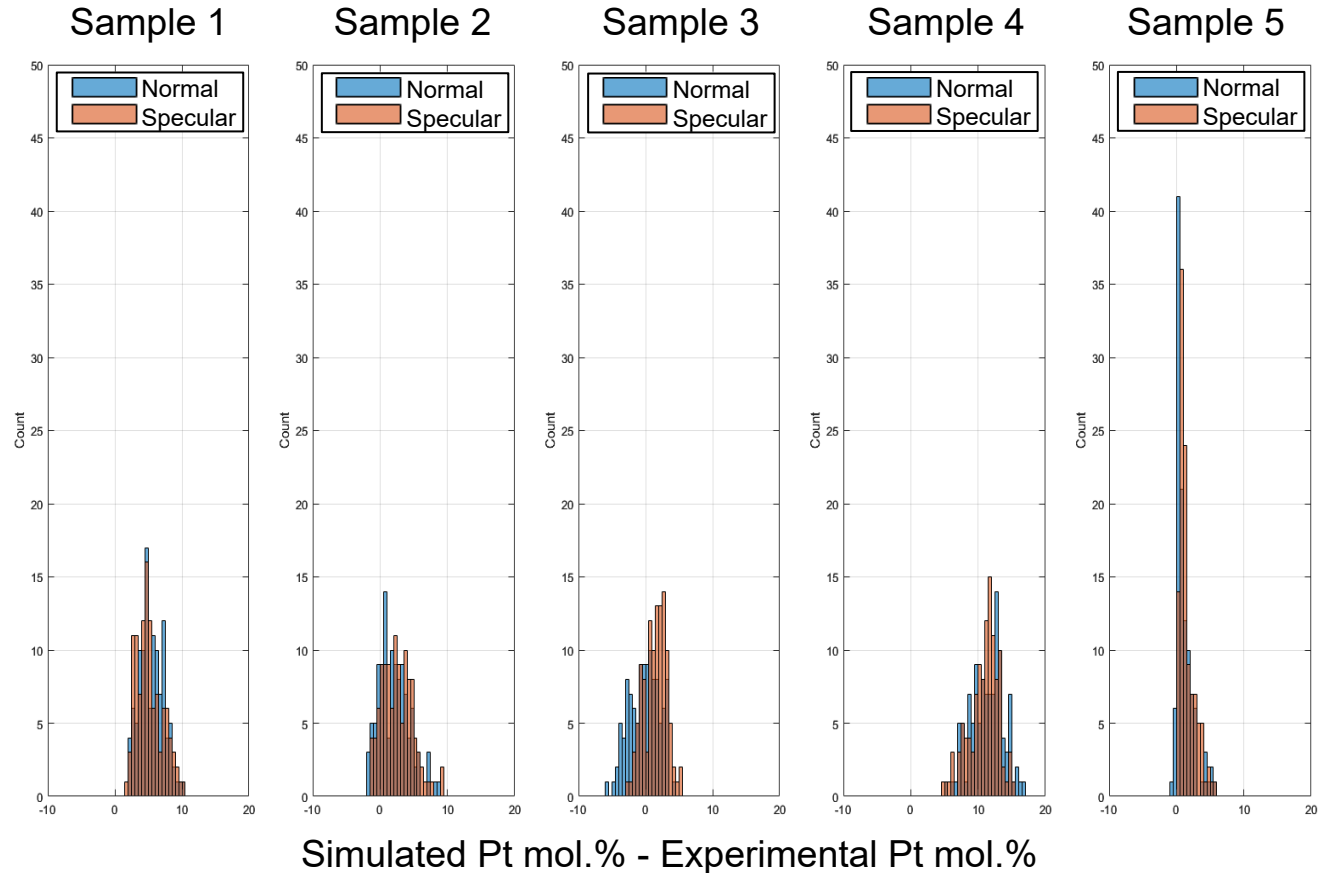
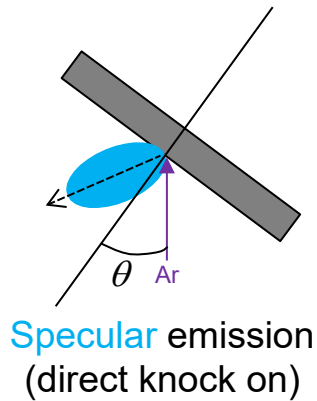
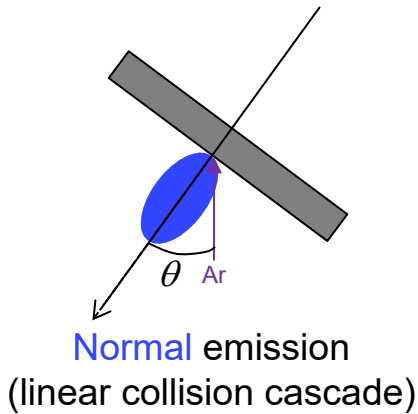
WDS involved a JEOL 8530 Hyperprobe w/5 spectrometers.

EPMA software provides fully automated, programable data collection method for all standards and sample locations.

With pre-developed routine, data reduction and output can be < 1 hr analyst-interaction time.

WDS uncertainty estimated at 4-5 mol.% This slightly higher than normal value attributed to charging.

Detailed SIMTRA simulations considered the potential impact of normal vs. specular emission on film composition.

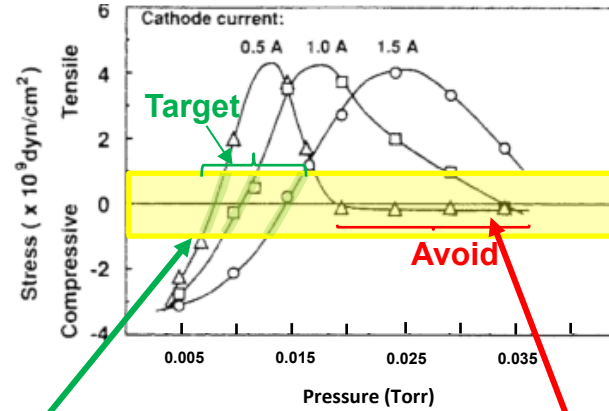


No better matching to experimental compositions when considering specular vs. normal emission of ejecta.
Comparison across 5 depositions (560 characterized areas).

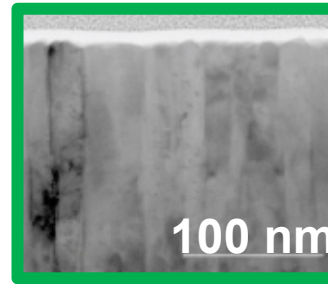
Early BayesOp success shows optimal conditions for low film stress, large density, low resistance, and robust process.

Longstanding problem with 'stressy' thin films.

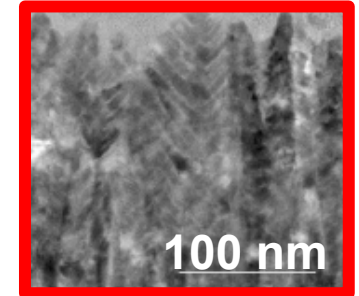
- desire low stress to avoid failures (delamination).
- desire dense film which corresponds **Target** region exhibiting rapid change from compressive to tensile.
- desire low film resistivity.
- desire robust process: minimize impact of inevitable, slight process variations (like pressure).



Residual stress vs. argon pressure used during deposition (N.N. Josad et al. J. Vac. Sci. Technol. A 2001).



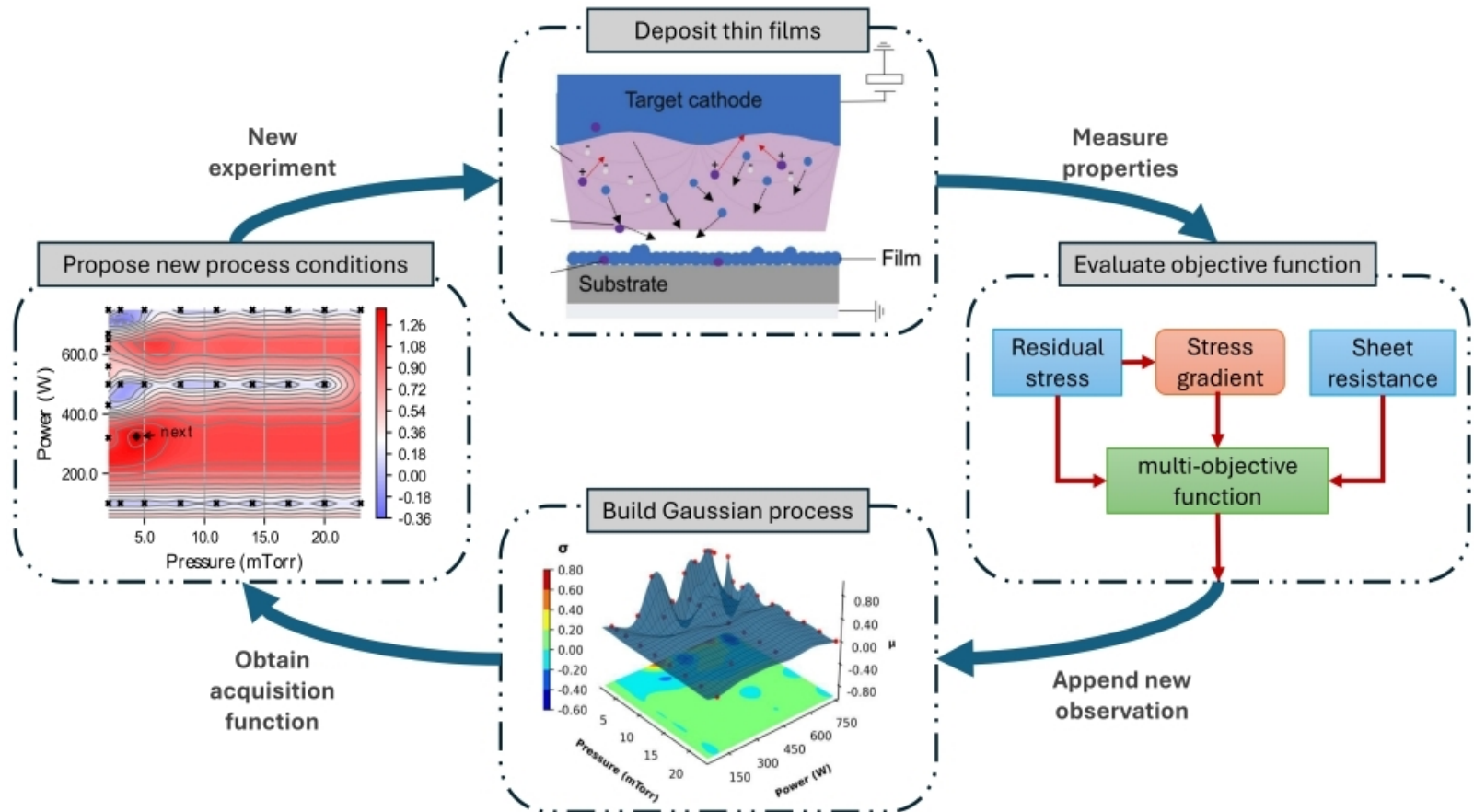
Dense, columnar microstructure



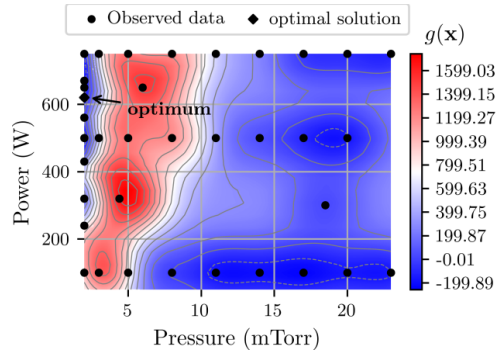
Under dense, branched microstructure

Bill Westwood in *Sputter Deposition* (2003):
“Because of the rapid change from compressive to tensile, it may not be practical to obtain a low stress by controlling the pressure.”

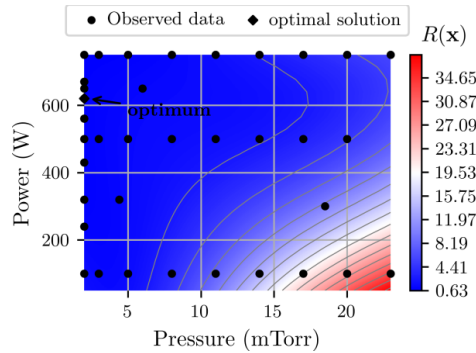
Open-loop Bayesian Optimization with iterative sputter deposition has identified optimal conditions for low stress, large density, low resistivity films made by robust process.



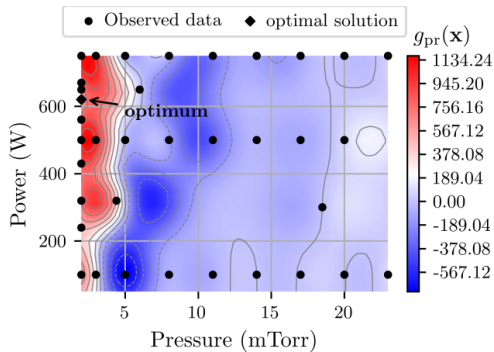
Early BayesOp identified optimal process conditions for low stress, large density, low resistance thin Mo film fabricated by a robust process.



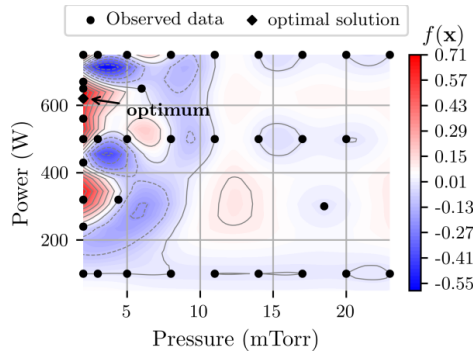
Stress at optimal loc. is between [-300, 300] MPa



Resistance at optimal loc. is < 3 mTorr

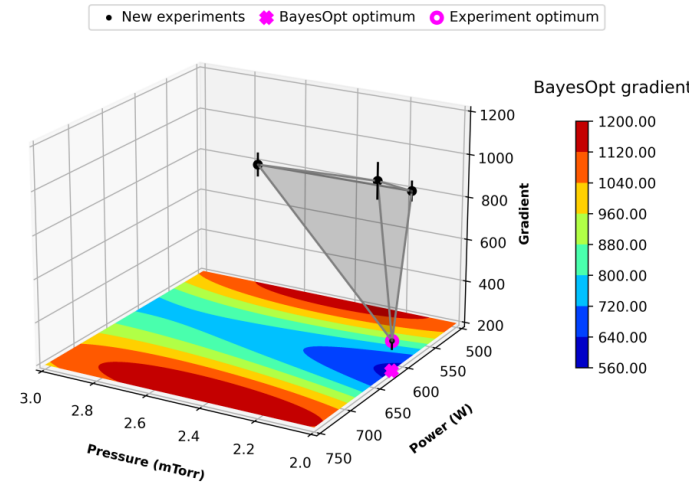


Stress gradient at optimal loc. is positive



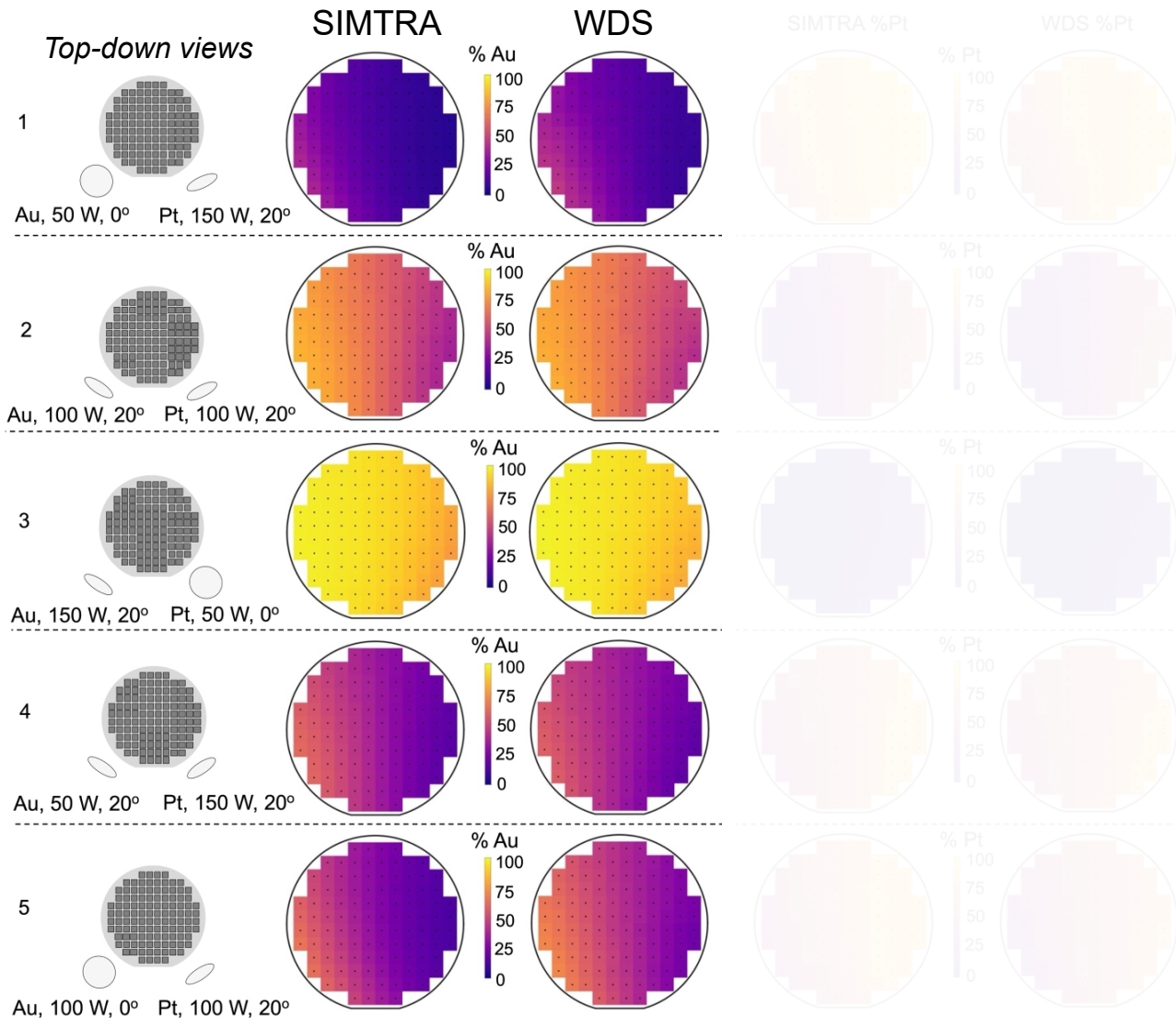
Stress gradient at optimal loc. is minima

Follow on experiments demonstrated that that the BayesOpt-identified process conditions are associated with a minimum stress gradient with pressure".



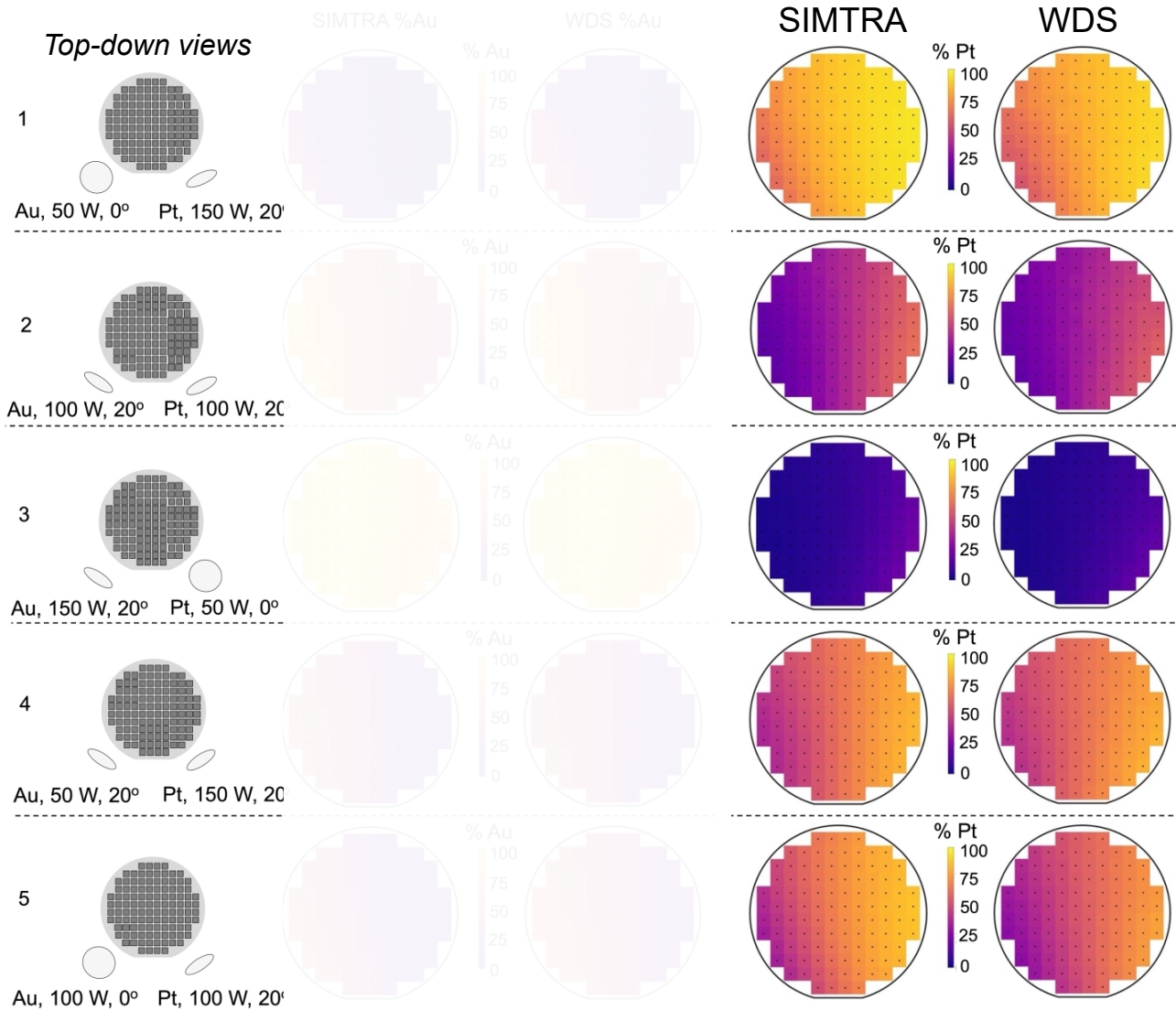
Follow on experiments verified a local minimum slope.

SIMTRA-predicted compositions closely match values measured by Wavelength Dispersive Spectroscopy (WDS).



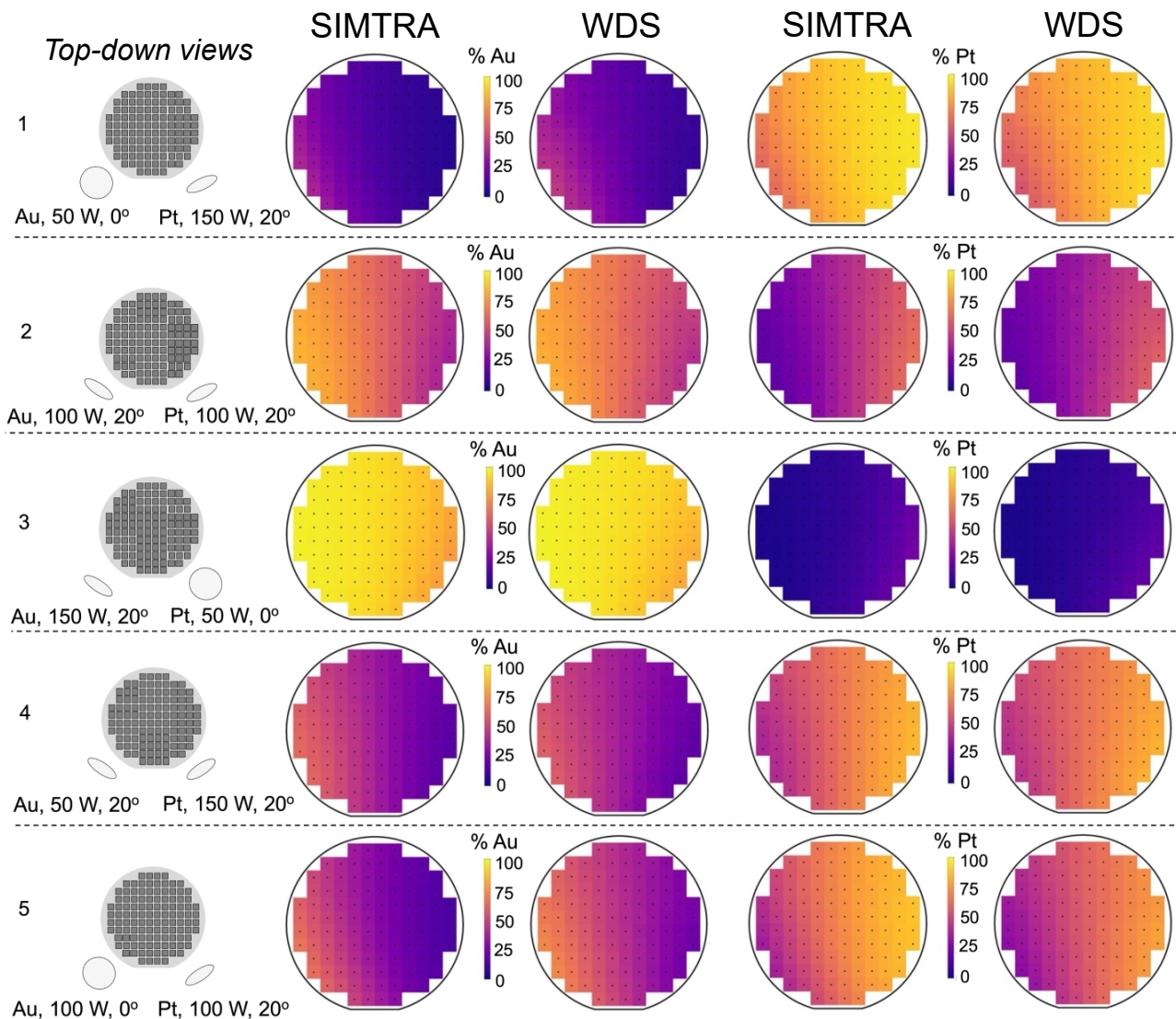
SIMTRA-predicted compositions are within 5 mol.% of WDS-measured values which is the uncertainty of these measurements.

SIMTRA-predicted compositions closely match values measured by Wavelength Dispersive Spectroscopy (WDS).



SIMTRA-predicted compositions are within 5 mol.% of WDS-measured values which is the uncertainty of these measurements.

SIMTRA-predicted compositions closely match values measured by Wavelength Dispersive Spectroscopy (WDS).



SIMTRA-predicted compositions are within 5 mol.% of WDS-measured values which is the uncertainty of these measurements.